Aggregation-Induced Emission Photosensitizers:

From Molecular Design to Photodynamic Therapy

Jun Dai, [†,#] *Xia Wu,* [‡,#] *Siyang Ding,* [§,#] *Xiaoding Lou,* [†,*] *Fan Xia,* [‡] *Shixuan Wang,* [†] *and*

Yuning Hong [§,*]

[†] Department of Obstetrics and Gynecology, Tongji Hospital, Tongji Medical College,

Huazhong University of Science and Technology, Wuhan, 430030, China

[‡] Engineering Research Center of Nano-Geomaterials of the Ministry of Education, Faculty of

Materials Science and Chemistry, China University of Geosciences, Wuhan, 430074, China

[§] Department of Chemistry and Physics, La Trobe Institute for Molecular Science, La Trobe

University, Melbourne, VIC 3086, Australia

ABSTRACT. Photodynamic therapy (PDT) has emerged as a promising noninvasive treatment option for cancers and other diseases. The key factor that determines the effectiveness of PDT is the photosensitizers (PSs). Upon light irradiation, the PSs would be activated, produce reactive oxygen species (ROS) and induce cell death. One of the challenges is that traditional PSs adopt a large flat disc-like structure, which tend to interact with the adjacent molecules through strong π-

π stacking that reduces their ROS generation ability. Aggregation-induced emission (AIE) molecules with a twisted configuration to suppress strong intermolecular interactions represent a new class of PSs for image-guided PDT. In this Mini Perspective, we summarize the recent progress on the design rationale of AIE PSs and the strategies to achieve desirable theranostic applications in cancers. Subsequently, approaches of combining AIE PS with other imaging and treatment modalities, challenges and future directions are addressed.

INTRODUCTION

Cancer is one of the leading causes of global death and remains a major health concern across the world. Conventional cancer treatment modalities such as surgical removal, radiation, and chemotherapy have substantial limitations like invasiveness or undesirable adverse effects, which prompts researchers to continually strive for better therapeutic options.[1] The most recently developed immunotherapy holds promise as a next-generation cancer therapy but still has its own problems such as the risk of autoimmune disorders. On the other hand, photodynamic therapy (PDT) has emerged as an alternative for cancer treatment because it is a non-invasive modality with high selectivity and low side effects.[2] The core of this technique is the photosensitizer (PS), which transfers photon energy to surrounding oxygen molecules to produce ROS in particular singlet oxygen ($^1O_2$) that cause cell death.[3] As the cytotoxicity of PS is activated by light, PDT represents a more manageable and controllable therapeutic option.[4] Moreover, as most of the PSs also have the ability to fluoresce, PDT offers a unique advantage of acting as both the therapeutic and image contrast agent at the same time, which allows the identification of cancerous lesions and monitoring of the therapeutic effect during the treatment.

A number of PSs have been developed so far to facilitate PDT. Even though several PSs have been clinically approved, developing new PSs with high tumor specificity, low toxicity in the dark state and high cytotoxicity upon light activation remains challenging.[5–7] One of the reasons is that traditional PSs, such as porphyrin, phthalocyanine, and analogs, adopt large flat disc-like structures, which are prone to aggregate and thus lead to the reduction of ROS generation ability and fluorescence quenching, i.e. aggregation-caused quenching (ACQ; **Figure 1A**).[8] Rendering the PSs water-soluble is one of the strategies to alleviate the aggregation issues but also induces other problems such as poor cell permeability. To suppress the unwanted formation of photoinactive aggregates such as H-aggregates, approaches including incorporating metal coordination, introducing bulky substituents, or adopting unique fabrication process to control self-assembly, have been reported to effectively enhance PDT efficacy through photoactive aggregate formation.[9,10] Different from classic PSs, AIE molecules adopt a twisted propeller shaped conformation, which suppresses strong π-π stacking in the aggregate state (**Figure 1A**).[11] Instead of fluorescence quenching for most of the conventional fluorophores, the AIE molecules become highly emissive in their aggregate/solid state due to the mechanism of restriction of intramolecular motions/rotations (RIM/RIR). Since the discovery of the unusual AIE phenomenon by Tang in 2001,[12] AIE-active molecules have been utilized in many areas ranging from optoelectronics, environmental sensing, bioimaging to theranostics. With strong fluorescence efficiency, large Stokes shift, good biocompatibility and resistance to photobleaching, AIE fluorogens (AIEgens) represent promising contrast agents across different imaging modalities in cell and animal models.[13] Through molecular design and engineering, the AIEgens exhibit strong photosensitizing ability that show the promise for cancer treatment, bacterial killing and image-guided therapy.

In this Mini Perspective, we will give an overview of the current development of AIE photosensitizers with highlights on their molecular design strategies and rationales. We will first introduce AIE PSs based on small molecule AIE scaffolds, AIEgens functionalized with targeting moieties through covalent bonds and those through non-covalent interactions. The emphasis will be on the strategies to achieve high $^1O_2$ generation efficiency and selectivity for cancer cells and tumors in vivo. Combining AIE PSs with other therapeutic modalities including chemotherapy, photothermal therapy, gene therapy through bioconjugation and nanofabrication to improve the therapeutic efficacy and to afford image-guided therapy will be discussed. Last, we will shed light on the current limitation, challenges and future opportunities in the area.
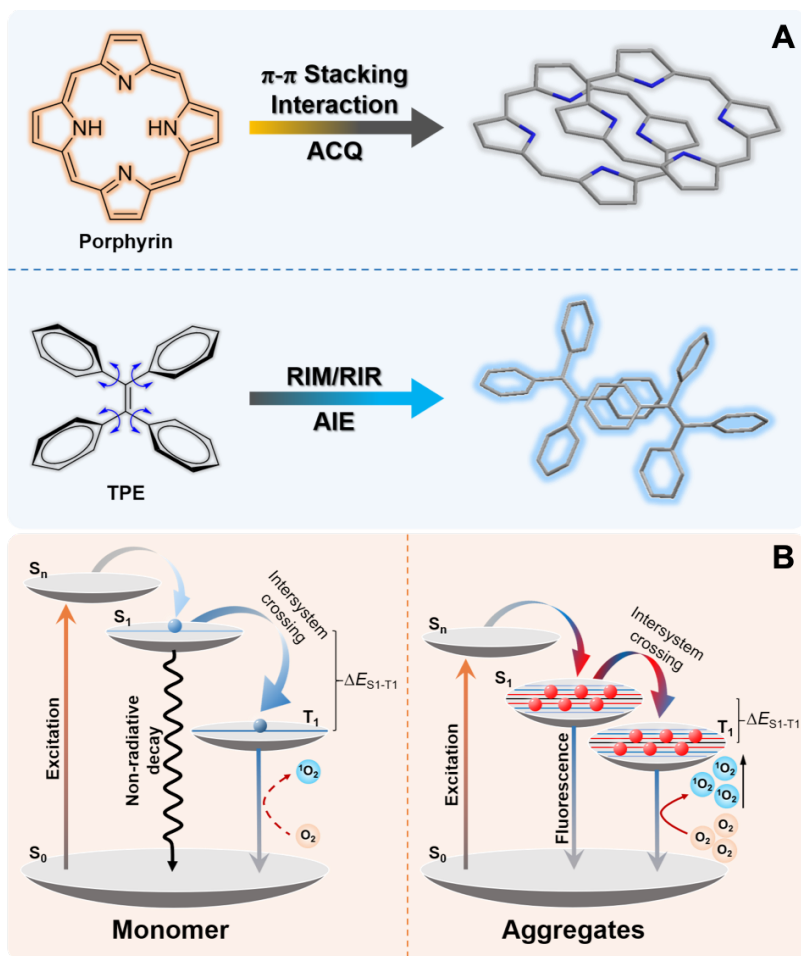
Figure 1. Schematic diagrams illustrating (A) fluorescence quenching of traditional PSs such as porphyrin in their aggregate states vs. fluorescence turn-on effect of AIE fluorogens such as tetraphenylethene (TPE) upon aggregate formation; (B) electron transitions of AIE PSs in their molecularly dissolved state (monomer) vs. aggregate state (aggregates). Note: energy levels are not in scale.

GENERAL STRUCTURAL DESIGN OF AIE-PS

AIE-PSs based on small molecule AIEgens are in particular useful for the study of structure-activity relationship and mechanism of action in cell death. When molecularly dissolved in solution, the nonradiative decay of AIE PSs is the major pathway due to active intramolecular motions/rotations, while upon aggregate formation, such processes are inhibited, and the excited state can thus be harvested for fluorescence as well as ROS generation (**Figure 1B**). The generation of the most cytotoxic $^1O_2$ relies on the energy transfer between the PS at the excited triplet state (T_1) and the molecular oxygen.[14] The prolonged lifetime for the triplet state allows sufficient time for the collisional transfer of energy to the adjacent oxygen molecule $(^3O_2)$, which leads to the formation of reactive $^1O_2$ and the PS relaxed back to the ground state. On the basis of this theory, reducing the energy gap between the lowest excited singlet state (S_1) to T_1 (ΔE_{S1-T1}) to facilitate the intersystem crossing process would be a strategy to endow AIEgens with PS capability (**Figure 1B**).[15,16] For most of the AIE PSs, introducing strong electron-donor and electron-acceptor pair(s) with π spacers in between could effectively change ordinary light-emitting AIEgens to AIE PSs. Meanwhile, introducing strong electron withdrawing units can also significantly red shift the emission of the AIE molecules possibly to the near infra-red (NIR) region. The AIE PSs with broad absorption spectrum and emission spectrum in the NIR region show extraordinary light harvesting

efficiency and have been demonstrated to nearly double their $^1O_2$ production efficiency than their counterparts emitting in shorter wavelengths.[17]

Organelle targeting AIE-PSs and their roles in PDT. Targeting key intracellular organelles that regulate the apoptosis pathway can enhance the efficiency of the PSs.[18]The impact of different organelle targeting AIE-PSs and their roles in inducing cell death as well as in vivo applications are summarized in **Figure 2**.
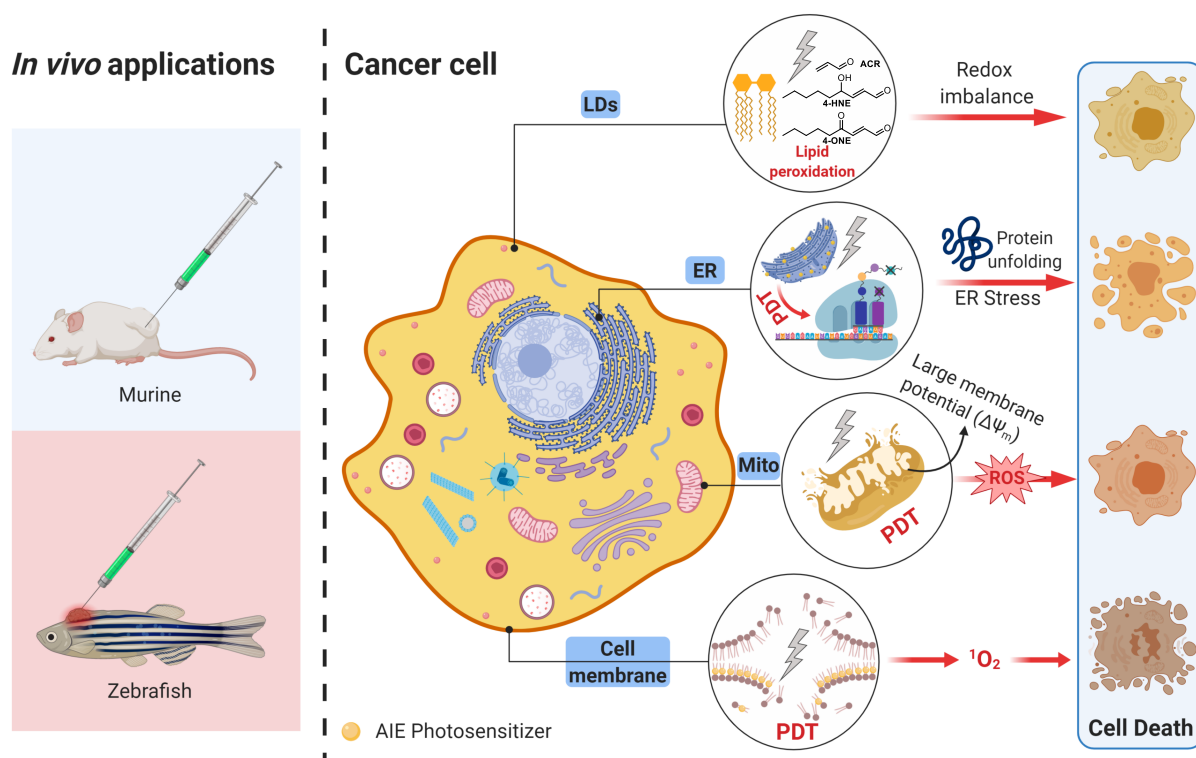
Figure 2. Schematic diagrams showing organelle-targeting AIE PS to regulate cell death.

Mitochondria, the powerhouse of the cell, are the major location of intracellular ROS production that mediates cell death signaling.[19] Meanwhile, cancer cells have a more negative mitochondrial membrane potential than normal cells. Such a hyperpolarized environment also allows mitochondria-targeting drugs to selectively accumulate in cancer cells but not in normal

cells.[20] Therefore, mitochondria represent an ideal target for various anticancer drugs. The pyridinium cation is a strong electron-withdrawing group commonly used as part of the AIE-PS building block (**Figure 3**). Tang and co-workers reported MeTTPy (**1**)[21], an AIE-PS based on triphenylamine-thiophene as the electron donor and pyridinium as the electron acceptor. **1** exhibits a broad absorption across the visible light region and strong emission which peaks at 669 nm in its aggregate state. With the aid of the pyridinium salt, it can penetrate the cell membrane and accumulate in the mitochondria region selectivity in cancer cells as evidenced by the fluorescence intensity measured in different cell lines. With negligible to low cytotoxicity in the dark, **1** exerts strong phototoxicity to cancer cells (e.g. A431 human epidermoid carcinoma cell line) but not normal cells (e.g. HLF human lung fibroblasts). Under white light irradiation, the $^1O_2$ generation efficiency of **1** was evaluated to be 90.7%, while commercial PDT PSs Ce6 and Rose Bengal only possess 16.7 and 55.6% respectively, by using the bleaching rate of 9,10-anthracenediyl-bis(methylene)dimalonic acid (ABDA) as an indicator. Subsequently, **1** was tested on A431-skin-tumor-bearing nude mice, which showed remarkable tumor retention properties and suppression of tumor proliferation activity upon white light irradiation (18 mW cm^{-2} for 10 min) by using Ki67 as the marker.
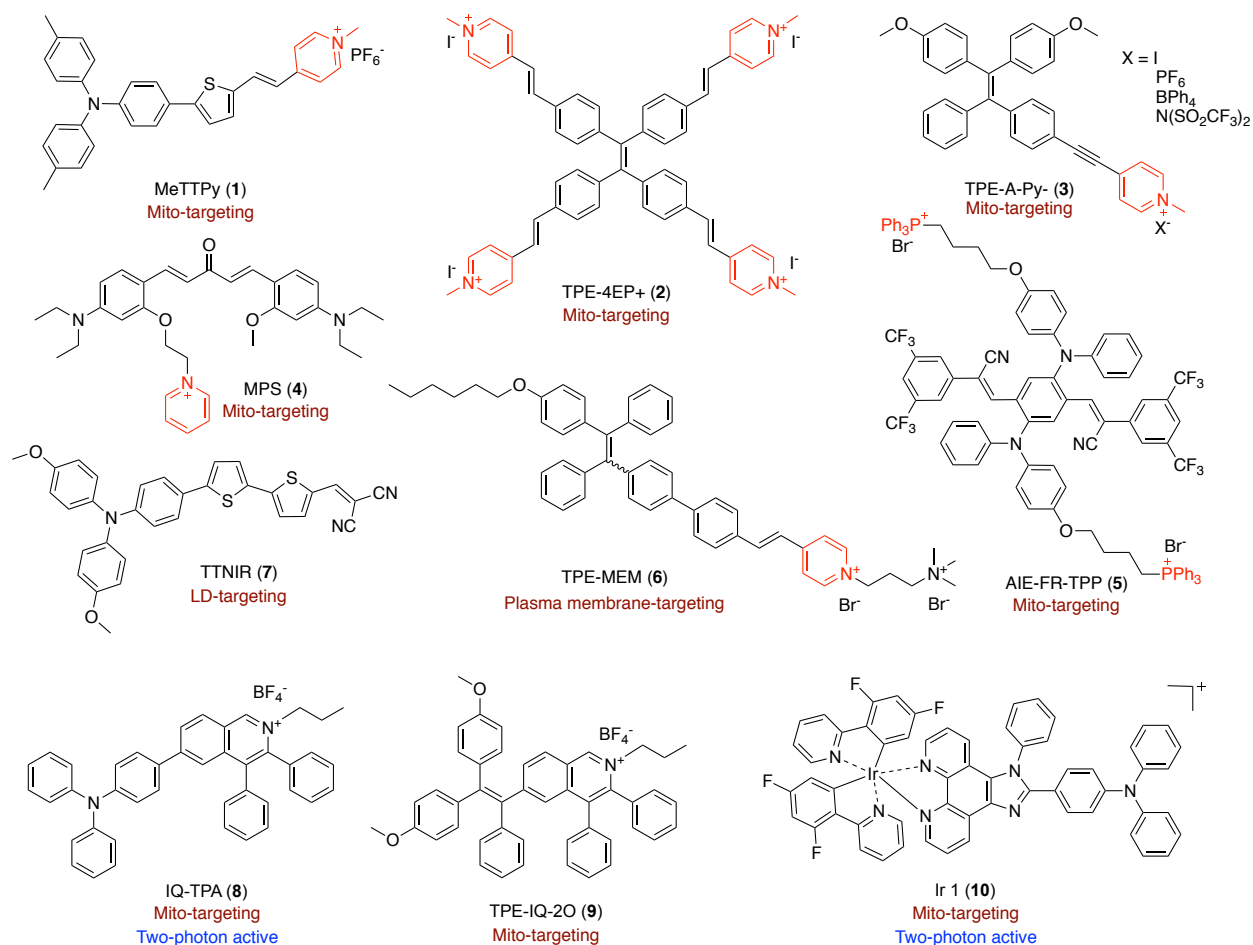
Figure 3 Chemical structures of organelle targeting AIE-PSs.

Similarly, TPE-4EP+ (**2**) with four pyridinium salts shows high ROS production efficiency with light activation.[22] TPE is a typical AIEgen that has attracted a lot of research attention. Interestingly, with a strong affinity to nucleic acids, **2** translocates from mitochondria to the nucleus when cells are in the late stage of apoptosis with compromised nuclear membrane integrity. Hence, it can be used to monitor the PDT process with real-time diagnosis to avoid excessive phototoxicity and thus minimize side effects. By altering the counterions, Zhang et al. demonstrated that heavy atom such as iodine (TPE-A-Py$^+$, **3**) can improve the photosensitization effect of pyridinium AIEgens.[23] Yang et al. demonstrated that even a pyridinium salt that is not

directly conjugated to the PS unit (MPS, **4**)[24] can contribute to photo-activatable ROS generation. Guo et al. showed an alternative approach of using triphenylpholinium (TPP), a mitochondria-targeting functional group, to direct AIE-PS (AIE-FR-TPP, **5**)[25] to the mitochondrial region and studied **5** in a zebrafish model.

Subcellular localization of the PSs can largely influence the signaling pathways that lead to cell death. While ROS generation locally in mitochondria usually leads to apoptosis, cells are predisposed to necrosis when PSs bind to the plasma membrane. Amphiphilic TPE-MEM (**6**)[26] with long alkyl chain are prone to anchor on plasma membrane. With the conjugation of the fluorogen to the pyridinium salt, even under room light activation, **6** is capable of promoting $^1O_2$ generation that oxidizes unsaturated phospholipids, cholesterol and membrane proteins and thus leads to the loss of membrane integrity. The fluorescence of **6** allows real-time visualization of membrane blebbing, cell swelling, the process that indicates cell death. The size of subcutaneous melanoma tumors implanted in nude mice shrank gradually following intratumoral injection of **6** twice a week with daily 30-minute exposure to laser irradiation.

Other organelles, such as lipid droplets (LDs) and the endoplasmic reticulum (ER), are also promising targets for PDT but yet to be explored. Recent studies have revealed the critical roles of LDs in cancer progression, survival and resilience to stress on top of their well-known function for lipid storage.[27,28] Neutral and hydrophobic AIE-PS TTNIR (**7**) specifically accumulates in LDs in the cellular milieu.[29] Triggered by white light, **7** produced ROS that possibly lead to lipid peroxidation, further propagation to other biomolecules and eventually cell death. On the other hand, ER-localized PSs can disrupt redox homeostasis to induce ER stress that activates apoptosis regulated by the collective network of the unfolded protein response. BODIPY derived PS with

ER-targeting glibenclamide exhibits promising phototherapeutic effects and could be used as a prototype for future AIE-PS design.[30]

Small molecule AIE-PSs for two photon PDT. AIE PSs activated by short wavelength in the UV or visible light region suffer from low penetration depth and potential photodamage to healthy tissues.[13] Shifting the excitation of AIE molecules to the long wavelength region would not be trivial when the inherent twisted structures are required for retaining AIE properties. Simply extending the conjugation system could result in synthetic difficulty, poor solubility and cell impermeability. In general, it is difficult for one-photon excitation to go beyond 750 nm to efficiently trigger $^1O_2$ generation. Two-photon excitation using far-red/NIR light can penetrate tissues more efficiently because of lower scattering and absorption by biological molecules in that region. Meanwhile, the multiphoton excitation process is nonlinear and occurs only at the focal point of the laser beam, which minimizes the out-of-focus photodamage (**Figure 4A**). Molecules with a large two-photon absorption (2PA) cross-section are desired for such applications. Different approaches have been adopted to improve the 2PA cross-section, including designing molecules with symmetric charge transfer from the ends to the middle of a conjugated system, encapsulating dyes in nanoparticles to construct energy-transferring cassettes, and others.[31] These strategy could potentially be implemented in the design of two-photon excitable AIE PSs.
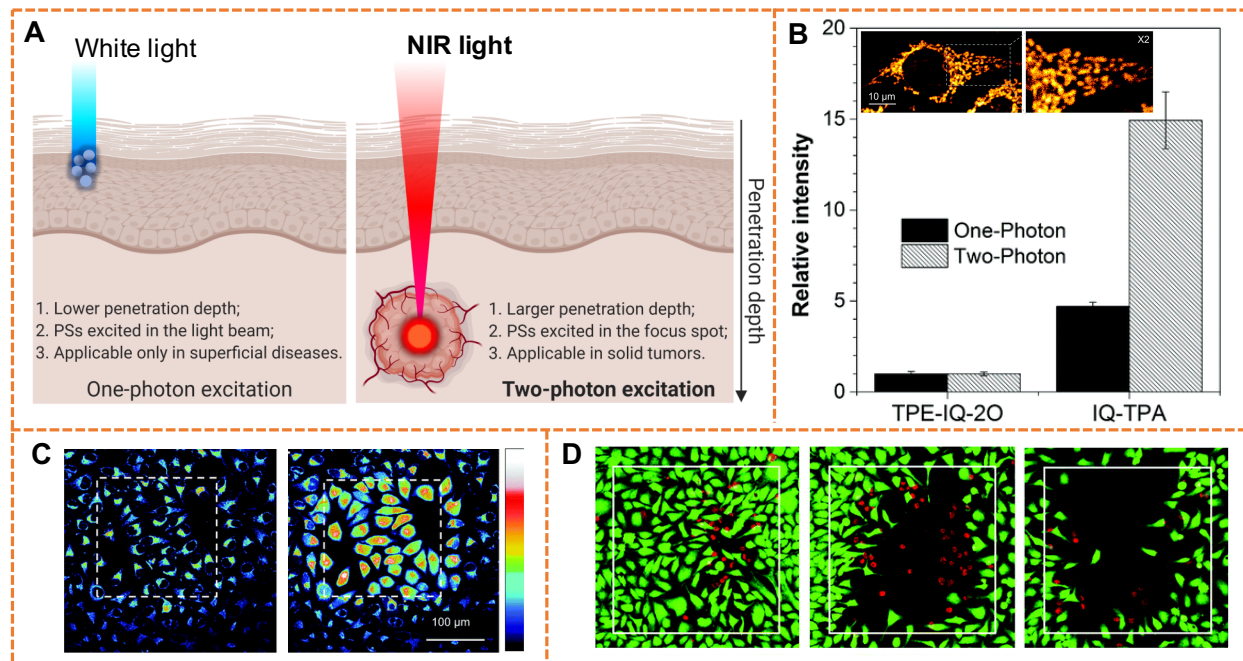
Figure 4 Two-photon excitation in PDT. (A) Comparison of one-photon and two-photon excitation. (B) Relative fluorescence intensity of IQ-TPA (2PA-active) and TPE-IQ-2O (2PA-inactive) with one- or two-photon imaging. Inset: mitochondria of HeLa cells stained by IQ-TPA under two-photon PDT. (C) Intracellular ROS generation induced by IQ-TPA upon photo-irradiation, revealed by DCFH-DA fluorescence. (D) PDT effect of IQ-TPA assessed by fluorescein diacetates (green; live cells) and propidium iodide (red; dead cells). Reproduced from ref (32). Copyright 2018 The Royal Society of Chemistry.

Tang and co-workers reported a mitochondrial AIEgen, IQ-TPA (**8**), for two-photon PDT.[32] IQ-TPA possesses a large 2PA cross-section (213 GM) at 900 nm in the NIR region. Compared to the TPE counterpart TPE-IQ-2O (**9**)[32], which is 2PA inactive, IQ-TPA exhibited similar brightness upon one-photon excitation but much higher intensity upon two-photon excitation (**Figure 4B**). With a lipophilic positive charge, IQ-TPA was found to target mitochondria selectively in cell imaging (**Figure 4C**). Intracellular ROS generation upon two-

photon excitation at 900 nm can be visualized by using a ROS activated fluorogen DCFH-DA (**Figure 4D**). The PDT efficiency of IQ-TPA was further evaluated by using a propidium iodine (PI) with red fluorescence to indicate dead cells and fluorescein diacetates (FDA) with green fluorescence to visualize live cells (**Figure 4E**). With the increase of scanning circles, more cells in focus were dead and became PI positive. The light dose required to kill 50% of the cells was calculated to be 3.7 kJ/cm^2 (8 mW, 387.5 × 387.5 μm^2), comparable to the value for porphyrin derivatives with a large 2PA cross-section (2.7 kJ/cm^2, 6.8 mW, 230 × 230 μm^2).

On the other hand, AIE-active metal complexes are also promising materials for two-photon PDT. Cao et al. studied the one-photon and two-photon PDT effect on a series of Ir(III) complexes, in which Ir-1 (**10**)[33] with 2-(2,4-difluorophenyl)pyridine (dfppy) as the ancillary ligand has a large 2PA cross-section (214 GM) excited by 730 nm light . **10** showed selectivity toward targeting and lighting up mitochondria. The perturbation of **10** to mitochondrial bioenergetics in cancer cells was evaluated on treated HeLa cells. Upon light irradiation, **10** led to suppression of mitochondrial respiration, pronounced impairments of oxidative phosphorylation as well as an impact on cytosolic glycolysis. Such effects were not observed in cells exposed to **10** without light activation. 3D multicellular tumor spheroids with extracellular matrix to hinder drug transport and create a hypoxic microenvironment were applied to mimic solid tumors. With two-photon excitation, **10** showed striking potency, with a low IC_{50} value to the spheroids, demonstrating its potential for PDT. More examples of AIE-PSs for two-photon PDT in vivo will be discussed in the latter sections.

IMPROVING PDT PERFORMANCE OF AIE-PS VIA COVALENT MODIFICATION

Nonspecific location of PSs could lead to unintended phototoxicity to normal cells and tissues upon exposure to light irradiation during PDT. To achieve the specific delivery of PS to diseased tissue, a number of strategies have been sought, for example, by using site-specific agents such as peptides, aptamers, or antibodies to carry the PSs to the target tissue. Alternatively, designing "caged" PSs that are only active by specific enzymes or microenvironment in cancers is another approach to improve the selectivity. On the other hand, traditional chemotherapeutic drugs usually lack specificity and thus often cause severe side effects. Combining chemotherapeutic drugs with PSs has advantages in cancer therapy, such as improving the controllability of the drug toxicity, allowing monitoring of the therapeutic effect (via PS fluorescence) and potentially overcoming drug resistance problem. Embedding the AIE-PSs in polymer chains essentially enables chemical modulation of the PS aggregation as well as easy modification of the entity to achieve specificity, pharmacological activity and therapeutic efficiency. In this section, we will exemplify the strategies adopted for improving the performance of AIE-PSs with the focus on covalent modification.

AIE-PS-peptide conjugates for PDT. Certain types of integrin receptors are tightly associated with cancers. For example, upregulation of $\alpha_v\beta_3$ and aminopeptidase N (CD13) receptors has been found in a wide range of cancer types, making them useful as neoplastic markers. Tripeptide with the sequence of Arg-Gly-Asp (RGD) and Asn-Gly-Arg (NGR) are found to selectively target $\alpha_v\beta_3$ and CD13 receptors, respectively, on the surface of cancer cells and thus have been extensively used to modify drugs, nanomaterials, etc. to achieve tumor specificity. Lou, Xia et al. attached a peptide fragment consisting of tumor targeted peptides (NGR and RGD), a cell-penetrating peptide (CPP) and a nuclear localization signal (NLS) peptide to an AIE-PS. The resulting TCNTP (**11, Figure 5**)[34] can bind to cells with CD13 and integrin $\alpha_v\beta_3$ on the membrane, being effectively

integrated into the cytoplasm and then delivered to the nucleus. Human malignant melanoma cells A374 (CD13 and $\alpha_v\beta_3$ expression cell line) showed the colocalization of TPE fluorescence with the nucleus stains, while breast cancer cells MDA-MB-231 ($\alpha_v\beta_3$ expression cell line) and fibrosarcoma cells HT-1080 (CD13 expression cell line) did not exhibit any TPE signals in the nucleus region. The results indicate that the peptide modification can selectively direct the AIEgens to the intracellular location of interest. Liu et al. has reported a dual activatable AIE-PS, TPETF-NQ-cRGD (**12**)[35], for image-guided PDT. In addition to cRGD tag, **12** contain the 2,4-dinitrobenzenesulfonyl (DNBS) moieties to mask the fluorescence and photosensitizing activity of the molecule, which can be selectively cleaved by high concentration of thiols such as glutathione (GSH) in the reducing intracellular environment of cancers. Upon binding to $\alpha v\beta 3$ receptors, **12** was internalized by endocytosis and the intracellular GSH removed the DNBS units to restore its photosensitizing and light emitting abilities. To enable the real-time monitoring of the AIE-PS therapeutic response, an additional responsive linker, -Asp-Glu-Val-Asp- (DEVD) peptide was incorporated in TPETP-SS-DEVD-TPS-cRGD (**13**)[36], which was cleaved by the enzyme caspase-3/-7 that are only active in apoptotic cells. The release of TPS unit aggregated and thus emitted strongly in the cells to report on the apoptosis, which reflected the therapeutic effect of the AIE-PS.

Apart from markers on cancer cell surface, proteases that selectively degrade extracellular and intracellular proteins are strongly associated to cancer progression, in particular invasion and metastasis.[37] Overexpressed proteases with concentration numerous folds higher have been identified in cancerous cells than in normal cells. Meanwhile, the acidic environment of tumors is usually favored for the activation of these proteases. Cathepsin B is a lysosomal protease overexpressed in breast, cervix, melanoma and many other types of cancers. Prodrug TPECM-

2(FGLGD$_3$-cRGD)[38] (**14**) incorporated multiple linkers with sequence of -Gly-Phe-Leu-Gly-(GFLG), which can be selectively cleaved by overexpressed cathepsion B to resume the photosensitizing ability of the AIE-PS. Matrix metalloproteinase-2 (MMP-2) is another target protease associated with cancers. A strategy of using MMP-2 responsive peptide (LGLAG) to link a DNA-binding anticancer drug, doxorubicin (DOX), with TPE derivative (DOX-FCPPsPyTPE, DFP, **15**)[39] has been demonstrated to achieve the controlled drug delivery and release in cancer cells but not in normal cells. The fluorescence of TPE enables the real-time tracking of this drug release process.

The trans-Golgi protein convertase furin has been reported to be overexpressed in cancers including non-small-cell lung cancer, glioblastomas and head and neck carcinomas. Liang et al. demonstrated the use of an acetyl-RVRR peptide to modify TPE (**16**).[40] In the presence of furin, cleavage of the peptide led to the aggregation of the TPE (medium fluorescence), which can consequently undergo condensation on the 2-cyanobenzothiazole unit to form a highly emissive dimer with dual TPEs. Zhang et al. decorated the TPE based PS, TPE-red-2AP2H (**17**)[41], with a peptide AP2H (IHGHHIISVG), which can selectively bind to the hydrophilic extracellular loop of lysosomal protein transmembrane 4 beta (LAPTM4B), a protein overexpressed in many solid tumors. While exerting almost no phototoxicity to normal cells, **17** can effectively cause the death of LAPTM4B overexpressed cells upon photoexcitation. The red fluorescence of **17** also allowed the real-time tracking of the translocation of LAPTM4B during cell death.

cNGR
Targeting CD13

CPP
Improving uptake

AIE-PS

NLS
Delivery to nucleus

RGD
Targeting integrin

R =

TCNTP (**11**)

AIE-PS

cGRD
Targeting integrin

DNBP as "cage"
Cleaved by GSH

TPETF-NQ-cRGD (**12**)

TPETP
AIE-PS

Cleaved by
glutathione (GSH)

Caspase cleavage site

TPS
AIEgen

cGRD
Targeting integrin

TPETP-SS-DEVD-TPS-cRGD (**13**)

TPECM
AIEgen/PS

R=

GFLG
Cathepsin B responsive

D3
Hydrophilic

cGRD
Targeting integrin

TPECM-2(GFLG-D3-cRGD) (**14**)

DOX
Chemodrug

Arginine-rich motif
Increasing hydrophilicity and cell penetration

LGLAG
Metalloproteinase-2 substrate

AIE-PS

DOX-FCPPsPyTPE (**15**)

Furin cleavage site

Dimer forming part

AIEgen

Acetyl-RVRR-TPE (**16**)

AIE-PS

TPE-red-2AP2H (**17**)

Targeting lysosomal protein transmembrane 4 beta

AP2H =

16

Figure 5 Chemical structures of AIE-PS-peptide conjugates used for PDT. The functions of the peptide segments are also shown.

AIE-PS-chemotherapeutic agent conjugates for PDT. Coupling chemotherapeutic drugs with AIE-PS enables the synergistic chemo-photodynamic therapy, while the fluorescence of AIEgens can also provide a window to monitor the controlled delivery and release of nonluminescent anticancer drugs as well as their therapeutic response. Liu et al. reported a system TPEPY-S-MMC (**18**)[42] in which the chemo-prodrug (Mitomycin C, MMC) acts as the quencher for both the photosensitizing and fluorescence properties of the PS (TPEPY-SH). Upon GSH activation, the active group on MMC was released to react with DNA, accompanied by ROS generation from the TPEPY-SH for combinational chemo-photodynamic therapy (**Figure 6A**). Upon intratumoral injection to 4T1 tumor bearing mice, red fluorescence from TPEPY-SH was gradually increased in the tumor area and remained the strongest among all the organs over 24 h, indicating the activation of the dual-prodrug in the reducing tumor environment. With white light irradiation, the tumor growth was largely suppressed in **18**-treated mice and the tumor tissue was severely damaged by the combination therapy. Chlorambucil (Cbl) is an antitumor agent that crosslinks DNA strands through alkylation to prevent the replication and transcription. Such alkylation can also occur non-specifically with proteins before the drug reaching their target location and thus leads to toxic side effects. Singh et al. adopted a TPE scaffold with 4 caged Cbl units (TPE(Cbl)$_4$, **19**)[43], which was non-toxic before photo-irradiation. Upon exposure to visible light, the aggregates of **19** in water became an active PS to induce $^1O_2$ generation, which in turn led to the release of active Cbls to further inhibit tumor growth. The process can be monitored by the green fluorescence from the aggregation of the TPE fluorogen. Artmisinin (ART) is a natural product that has recently been found to inhibit cell proliferation and angiogenesis by inducing oxidative

damage. Liu and coworkers have prepared a TPETH-Mito-1ART (**20**)[44], which contains a TPE-based PS, cationic sidechains to direct the dye to mitochondria, and an ART. The scaffold of **20** improved the specific targeting of both the AIE-PS and ART to mitochondria where they can work effectively and synergistically to induce cell apoptosis.
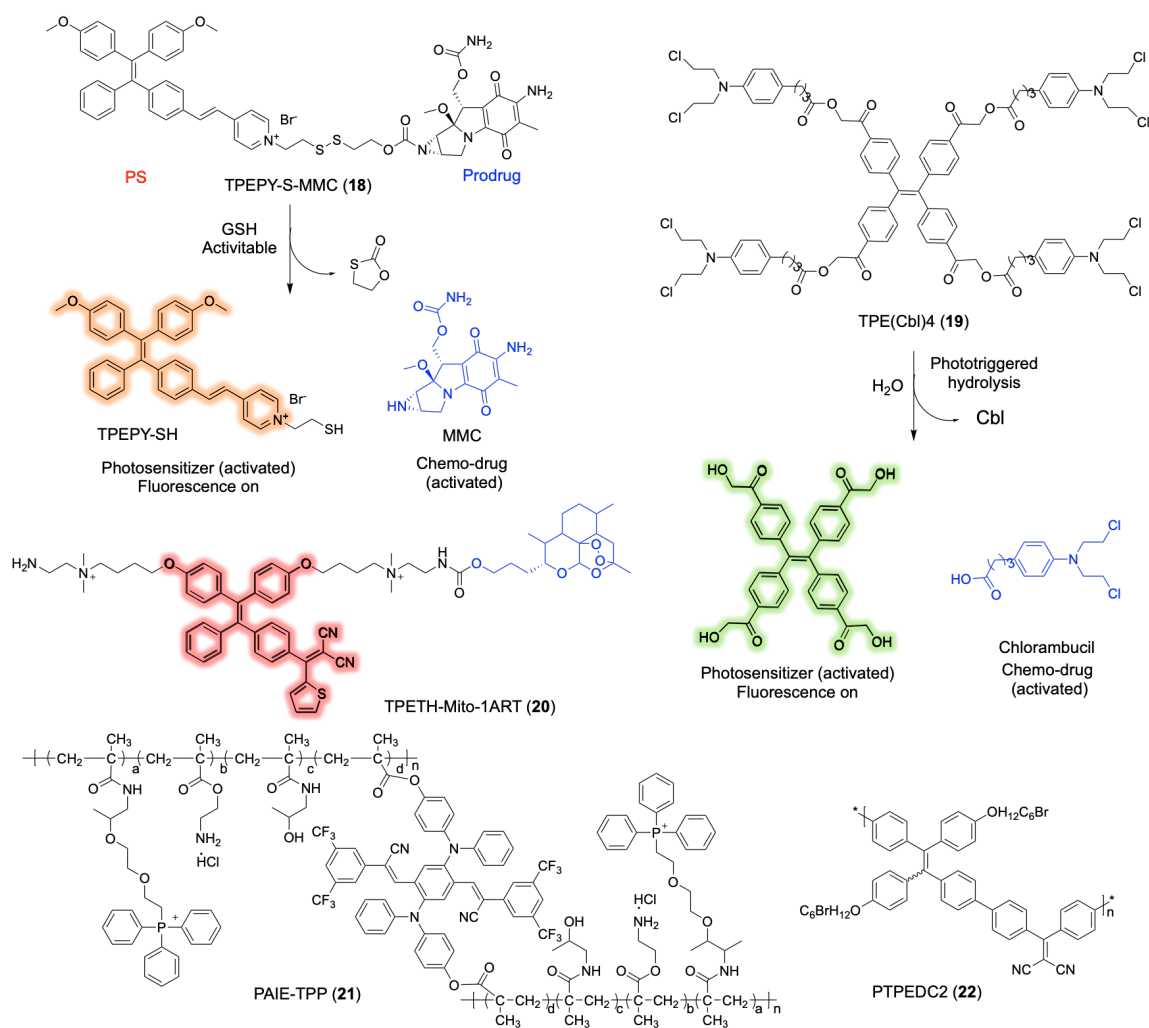
Figure 6 Chemical structures of AIE PS-chemodrug conjugates (**18-20**) and polymer-based AIE-PS (**21-22**). The proposed working mechanism for releasing chemotherepeutic prodrugs were shown.

Gao, Ren, Tang et al. presented a strategy of combining dual organelle targeting chemo-drug and PS to improve the therapeutic effect as well as to self-monitor the treatment process. Mitochondrial-targeting AIE chemotherapeutic unit, AIE-Mito-TPP,[45] spontaneously assembled with a lysosome-targeting conventional PS, AlPcSNa4 with opposite charges to form nanoparticles (NPs) with better cell permeability. After entering the cells via endocytosis, AIE-Mito-TPP escaped from lysosomes, accumulated in mitochondria and induced cell death through disturbing the mitochondrial membrane potential. Meanwhile, AlPcSNa4 localized in lysosomes and disrupted lysosomal functions when irradiated by NIR light. The therapeutic process can be visualized by confocal microscopy and quantified by flow cytometry through dye fluorescence. The system has been demonstrated to efficiently kill cancer cells in vitro and inhibit tumor growth in vivo in A375-bearing nude mice. In addition to combining with classic chemotherapeutic drugs, AIE-PSs have also been used in conjunction with siRNA for targeted PDT and RNA interference therapy. This will be discussed in the Combinational therapy section.

Polymer-based AIE-PS. Linking AIE-PSs together through covalent bond with certain polymers is a simple strategy to improve the stability and biocompatibility as well as their $^1O_2$ production efficiency. Gao and coworkers developed a copolymer including hydrophilic blocks and segments that are functionalized with the mitochondrial-targeting TPP. The core photosensitizing structure of **5** was used to crosslink the polymer to generate PAIE-TPP (**21**)[46] that can not only emit in the far-red/NIR region but exhibit better ROS quantum yield (up to 77.9%) upon light activation. Hydrophilic and biocompatible polyethylene glycol (PEG) has been used to decorate the AIE-PS salicylaldazine to afford its self-assembly ability to micelle nanostructure and thus improve cell uptake. Liu's group has discovered that conjugated polymer PSs exhibit a higher $^1O_2$ quantum yield, brighter fluorescence, and larger 2PA cross-sections than the corresponding monomeric

PSs.[47] The denser energy levels in both the singlet and triplet states may increase the probability of intersystem crossing and thus lead to higher $^1O_2$ generation efficiency. Compared to TPEDC, conjugated polymer PTEPDC2 (**22**)[47] exhibits a more than 5-fold increase of $^1O_2$ generation and 6-fold higher 2PA cross-section. The outstanding 2PA properties of PTEPDC2 have been used for in vitro cancer cell ablation and in vivo zebrafish tumor treatment.

IMPROVING PDT EFFICIENCY OF AIE-PS VIA NONCOVALENT NANOASSEMBLY

The above discussion suggests that target groups or adjuvants conjugated to AIE-PSs can improve their specificity, $^1O_2$ generation efficiency, as well as other properties such as two-photon excitation PDT. However, covalent modifications on the AIE-PSs can be nontrivial and whether the modification would change the original therapeutic and pharmacological properties of the adjuvant should be carefully examined. Alternatively, the emerging technology of noncovalent modification of AIE-PSs through incorporating different compartments into nanoparticles (NPs) holds advantages such as simple fabrication, long-term biocompatibility, and diverse functionality. The general strategy is to encapsulate hydrophobic AIE-PSs in an amphiphilic polymer matrix followed by surface modification by targeted group. The obtained PS-loaded nanostructures usually exhibit intense fluorescence and appreciable $^1O_2$ generation efficiency for image-guided PDT. In particular, amphiphilic 1,2-distearoyl-*sn-glycerol*-3-phosphoethanolamine-*N*-[maleimide(polyethylene glycol)] (DSPE-PEG-Mal) and analogues are commonly used as encapsulation matrix for AIE-PSs with the reactive group (e.g. maleimide) to further link peptide or other surface modification moiety (**Figure 7**). In this section, we will focus on the surface modifications of the nanoparticles for the targeted delivery of PS and the optimization of the matrix to enhance PDT efficiency.
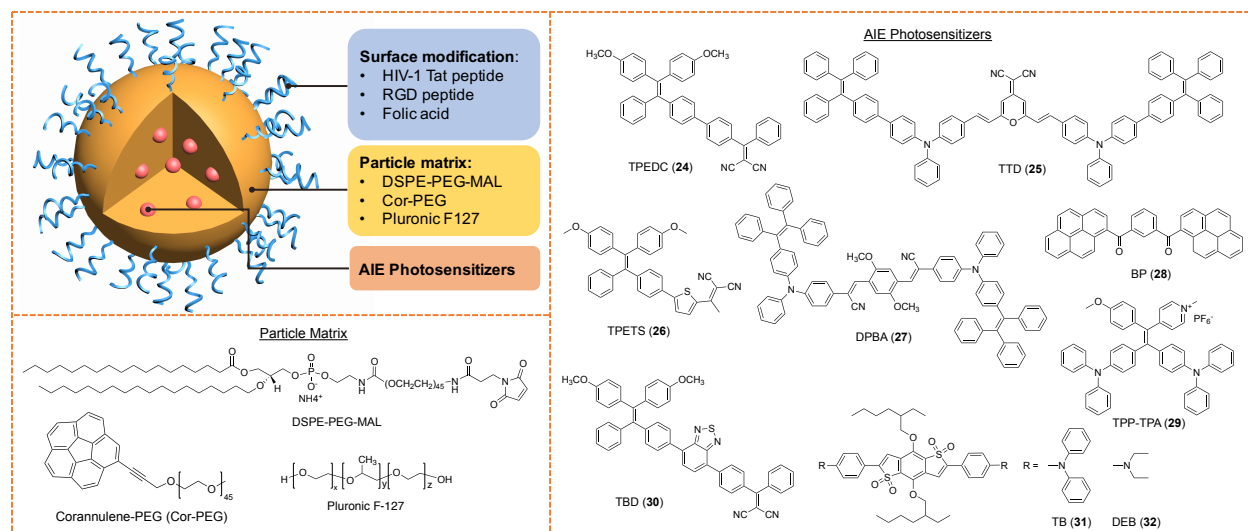
Figure 7. General strategy of AIE-PS containing nanoparticles for cancer theranostics. Examples shown for AIE-PS structures, encapsulating matrix for nanoparticle fabrication, and surface modification.

Surface modification to improve cell permeability. The human immunodefficiency virus (HIV)-1 derived transactivator of transcription (Tat) peptide is one of the most commonly used CPP for basic, preclinical and clinical research.[48] Liu et al. has reported using the HIV-1 Tat peptide (RKKRRQRRRC) to functionalize the surface of NPs containing TPETCAQ (**23**) as the PS and DSPE-PEG-Mal as the matrix.[49] While the most widely used PS such as Ce6, ICG and Rose Bengal are easily decomposed, the TPETCAQ NPs showed extraordinary stability and higher phototoxicity upon light irradiation. The NIR emission allowed in vivo image-guided therapy in tumor-bearing mice. After intratumoral infection and exposure to light for 5 min, TPETCAQ NPs efficiently generated $^1O_2$ to kill the luciferase transgenic 4T1 cancer cells. Proliferating cell nuclear antigen (PCNA) staining indicated that the proliferation capacity was largely reduced in TPETCAQ NPs treated tissue. Similarly, T-TPEDC dots were fabricated with TPEDC (**24**)[50] as the PS. T-TPEDC dots were stable in cell culture medium for 3 days while retaining the ROS

generation ability. With large two-photon cross section (3500 GM @ 850 nm), T-TPEDC dots allow the precise PDT action in deep tissues of mouse. Through tail vein injection, the brain vessels of the mice can be visualized by two-photon excitation. More significantly, the activation of the PDT effect of T-TPEDC dots can lead to the closure of blood vessels in the selected area, which lead to necrosis of the tumor as an effective cancer treatment (**Figure 8A**). This NP fabrication method is also applicable to organometallic complex as the PS. Multinuclear Ir(III) complex NPs[51] with an AIE feature represented the first example of multinuclear Ir complexes for enhanced PDT with excellent biocompatibility and therapeutic potential.

Surface modification to improve cancer cell targeting. As mentioned above, short peptides containing linear or cyclic RGD sequence are well known for their integrin-binding ability. Liu et al. reported nanoparticles with TTD (**25**)[52] embedded as the PS and surface modification of cRGD for the selective imaging and killing of cancer cells. Zheng, Liu and coworkers then applied the same NPs to tumor-bearing mice.[53] The uptake of TTD NPs by tumor tissues can be visualized by a noninvasive fluorescence imaging system, thanks to strong red emission from AIE NPs, which revealed the maximum accumulation of the NPs in tumor 8 h post-injection (**Figure 8B**). Cilengitide, which incorporates a cyclic RGD moiety, was used as a blocking agent to validate the specificity of TTD NPs to the tumor. After PDT treatment with TTD NPs and laser irradiation (532 nm, 250 mW/cm^2), obvious tumor shrinkage was observed after 3 days.
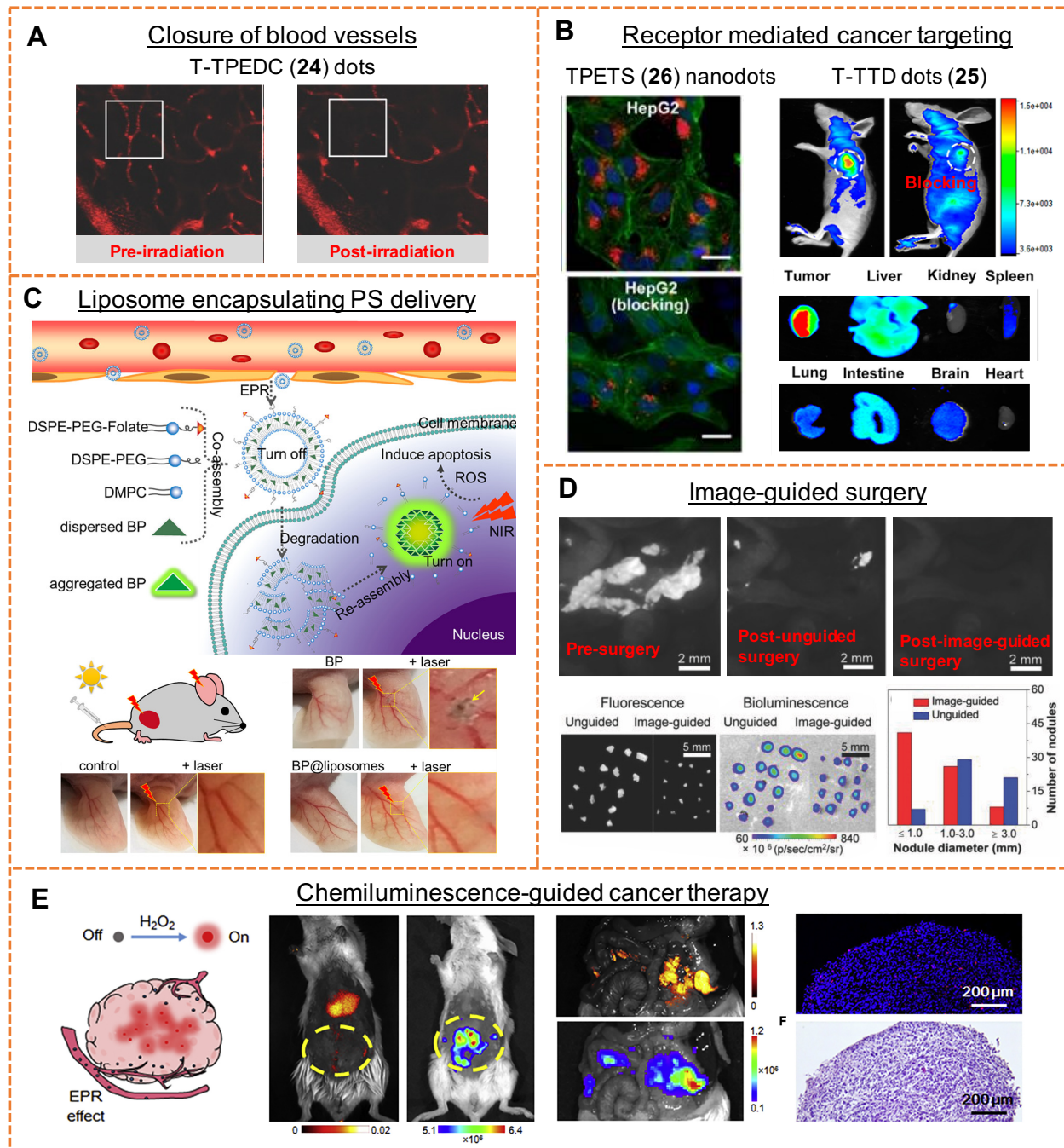
Figure 8. AIE-PS nanostructures for PDT applications. (A) The closure of brain vessels of mice treated with T-TPEDC dots after photoirradiation. Reproduced from ref (50). Copyright 2018 Wiley-VCH. (B) Left: Red fluorescence revealing the targeting of RGD peptide modified TPETS nanodots to HepG2 cells with over expression of integrin receptors. Reproduced from ref (54).

Copyright 2019 Ivyspring International Publisher. Right: Bio-distribution of T-TTD dots in tumor-bearing mouse 8 h post injection and fluorescence signals from various mouse organs 12 h after injection. Reproduced from ref (53). Copyright 2017 American Chemical Society. (C) Illustration of targeted delivery and activation of folate functionalized AIE-PS co-assembled liposomes (BP@liposomes) for PDT. Normal tissues such as blood vessels in mouse ears were severely damaged by BP nanoaggregates with laser irradiation but not BP@liposomes under the same conditions. Reproduced from ref (56). Copyright 2019 American Chemical Society. (D) Cor-AIE dots fluorescence improves the precision of surgical tumor removal. Fluorescence and bioluminescence images of nodules harvested from unguided and Cor-AIE dots fluorescence guided surgery were shown for comparison. Reproduced from ref (57). Copyright 2018 Wiley & Sons, Inc. (E) Left: Illustration of the C-TBD NP chemiluminescence activated by EPR effect in H_2O_2-enriched tumor microenvironment. Middle: in vivo abdominal metastatic breast tumor imaging by fluorescence (pseudo red hot color) and chemiluminescence (pseudo rainbow color) of C-TBD NPs. Right: Fluorescence imaging (red dots) and H&E staining to illustrate the distribution of C-TBD NPs in a slice of abdominal metastatic breast tumor. Reproduced from ref (58). Copyright 2017 Elsevier Inc.

A similar strategy was adopted in fabricating nanodots with TPETS (**26**)[54] as the PS by Li, Liu and coworkers. They first used immunofluorescence and RT-qPCR to confirm high level of $\alpha_v\beta_3$ expression in tissues from hepatocellular carcinoma patients and tumor-derived cell lines. Flow cytometry and confocal microscopy were then used to quantify the targeted uptake of the nanodots by cancer cells that overexpressed integrin. Upon receptor-mediated endocytosis, the nanodots accumulate in the lysosomes of cancer cells (**Figure 8B**). With light activation, TPETS led to the release of lysosomal proteases to the cytosol, mitochondrial damage, and activation of

downstream caspases as the markers of apoptosis. While the nanodots alone or laser treatment alone did not induce any impact on tumor growth, PDT by nanodots plus laser (450 nm, 250 mW/cm^2, 10 min) significantly ablated the tumor, inhibited tumor growth, and extended the survival of tumor-bearing mice. The systemic toxicity of the nanodots has been evaluated in live mice, including body weight loss, kidney function indicators, potential tissue damage, inflammation or lesions and H&E staining was examined, indicating that the nanodots are highly biocompatible in the absence of light activation.

Folic acid binds selectively to folate receptors (FR) with high affinity. FR are highly expressed on the surface of a wide range of solid tumor cells such as in pancreatic, breast, ovarian, and colorectal cancers. The expression in healthy tissues is only limited to placenta, kidneys, lung and choroid plexus. Modifying the surface of the nanostructures with folic acids is thus a strategy for targeted delivery of the nanostructures to tumor tissues through FR-mediated endocytosis. In 2015, Liu's group reported a simple and general approach to deliver AIE-PS for cellular and mitochondrial dual-targeted PDT. A red fluorescent AIE-active DPBA-TPE (**27**)[55] was used as the PS and encapsulated in the nanodots with folate and triphenylphosphine on the surface. Upon selective internalization into FR-positive cancer cells, the nanodots accumulate in mitochondria and direct the generation of ROS, as discussed above, effectively causes cell apoptosis.

More recently, Li, Wang et al. proposed a novel strategy to control the photosensitizing ability of AIE-PSs through a coassembled method. The AIE-PS, BP (**28**)[56], was monomerically dispersed in the hydrophobic lipid bilayer when coassembled with the lipid molecules, including DSPE-PEG-Folate, during the formation of liposomes (BP@liposome). In this scenario, both the light emission and the ROS generation ability of BP was inhabited. With folate on the surface, the AIE-PS liposomes can be selectively internalized by FR-positive tumor cells. During this process,

the liposome will be degraded, and the AIE-PS can be delivered into the cells and then aggregated to produce ROS effectively upon light activation (**Figure 8C**). The fluorescence increased the liposome degradation and BP aggregation, which can be utilized to monitor the PDT process. Such an approach minimizes the phototoxicity of the AIE-PS in normal tissues. When tested on normal ear tissues of mice, nanoaggregates of BP presented severe damage in the laser irradiated area, while for BP@liposomes, no obvious changes were observed upon light irradiation (**Figure 8C**). With a large two-photon cross section, the BP containing liposomes can also be excited by two-photon laser to improve the treatment death in PDT.

Modification of encapsulation matrix to enhance PS performance. 1,2-Distearoyl-*sn*-glycero-3-phosphoethanolamine-*N*-[methoxy(polyethylene glycol)-2000] (DSPE-PEG) is the most widely used encapsulation matrix for constructing AIE NPs. Tang, Ding et al. reported an effective strategy to further enhance AIE-PS fluorescence and ROS generation efficiency by replacing DSPE-PEG with corannulene-decorated PEG (Cor-PEG).[57] The bowl-shape corannulene possesses a large dipole moment, super-hydrophobicity and hyper-rigidity, which provides environmental rigidity and strong interactions with the "rotor-rich" AIE-PS. In this example, the intramolecular motions of TPP-TPA (**29**)[57] are restricted and strongly suppress the nonradiative decay of the AIEgens. The resulting Cor-AIE dots showed a 4-fold amplified fluorescence quantum yield and 5.4-fold enhanced ROS production efficiency, compared to the normal AIE dots with DSPE-PEG as the encapsulation matrix. Subsequently, Cor-AIE dots were injected into the peritoneal carcinomatosis-bearing mice for 24 h, followed by surgery on the mouse abdomen. With NIR fluorescence imaging, a surgeon was able to remove most of the intraperitoneal tumors with relatively large diameters (> 1 mm) (**Figure 8D**; unguided surgery). A second operation was performed with the guidance of Cor-AIE dots luminescence, from which the remaining small

tumors were completely removed (**Figure 8D**; guided surgery). All of the harvested tumor nodules displayed bioluminescence signals (luciferase-expressed tumor), indicating that Cor-AIE dots can indeed improve the precision of cancer surgery. Further application of white light (0.4 W cm^{-2}) on the tumor area following Cor-AIE dots treatment significantly extended the survival time. Hence, enhancing the intraparticle confined microenvironment represents an effective approach to improve the performance of AIE dots and boost the phototheranostic efficacy of AIE-PS in cancer treatment.

Polymer Pluronic F-127 is an amphiphilic triblock copolymer with excellent water solubility and biocompatibility. Liu et al. reported a chemiluminescence photosensitizing NPs (C-TBD NPs), with far red/NIR-emitting TBD (**30**)[58] as the AIE-PS, CPPO as a chemical excitation source to react with H_2O_2 to generate the chemiluminescence and subsequently excite TBD for $^1O_2$ generation (**Figure 8E**). A higher H_2O_2 level was found in certain types of cancer cells than normal cells. After intravenous administration by the breast-tumor bearing mouse, C-TBD NPs were found to accumulate in the tumor region owing to the enhanced permeability and retention (EPR) effect and exhibit chemiluminescence gradually upon activation by H_2O_2 in the tumor microenvironment. After 1.5 h following an intravenous injection of C-TBD NPs, strong chemiluminescence was activated in the tumor region, whereas no obvious fluorescence signal was observed, owing to the penetration depth of chemiluminescence over fluorescence (**Figure 8E**). With the skin and peritoneum removed, in vivo imaging revealed the coincident localization of both fluorescence and chemiluminescence on the abdominal metastatic breast tumor region, which was further confirmed by H&E staining (**Figure 8E**). Combining with FEITC, an anti-tumor drugs that induces H_2O_2 accumulation in tumor cells, further enhanced the chemiluminescence

image contrast and PDT effect. This study presented a novel strategy based on chemiluminescence for image-guided cancer therapy and could motivate more attention to future clinical translation.

COMBINATIONAL THERAPY BASED ON AIE-PS

In spite of the aforementioned strategies to improve PDT efficiency and minimize the side effect of AIE PSs and other PS systems, there are still many challenges of using PDT in clinical settings. Given oxygen is one of the key components in PDT, the oxygen-deficient (hypoxia) tumor microenvironment, especially in solid tumors, greatly inhibits the effectiveness of PDT. The stress response of tumor cells could further suppress the effect of the PSs. One of the most promising ways to address the issues is to combine different treatments to enhance the efficiency and lower the risk of recurrence. In this section, we will introduce combinational PDT therapy with chemotherapy, photothermal therapy and gene therapy. The focus will be on the design strategy of the AIE-PS to achieve multimodal therapeutic effects.

AIE-PS nanoparticles for photodynamic and chemotherapy. Chemotherapy remains the primary clinical treatment strategy for solid tumors after surgical resection. However, it suffers from limitations such as the occurrence of multidrug resistance, side effects from non-specific targeting, difficulty to be delivered to the tumor, etc. For PDT, on the other hand, the generated ROS can introduce gaps in between endothelial cells and improve the enhanced permeability and retention (EPR) effect for chemodrug treatment. The combination of PDT with chemotherapy thus holds promise to overcome the weakness of each individual treatment modality. One strategy to combine both is to covalently link a chemodrug with the PS, which we have mentioned in the previous section. Thus, we will focus on the non-covalent strategies in this section.

Lou, Xia et al. developed a polymeric prodrug nanoassembly that entrapped a red-emitting AIE PS, TB (**31**)[59], and was grafted with a paclitaxel prodrug through a reduction sensitive linker (TB@PMP). The release of the chemodrug paclitaxel can be achieved by the high intracellular concentration of reducing agents, in particular, GSH in tumor cells. After releasing, free paclitaxel would bind to microtubules and disrupt cell function. Meanwhile, the disassembly of the polymer micelles also led to the release of TB, which tend to bind to mitochondria and induce apoptosis following light activation. The in vivo mice experiment showed that TB@PMP micelles preferentially accumulated in the tumor region, as monitored by EPR, after intravenous injection. The intrinsic fluorescence from TB allowed image-guided therapy to monitor the therapeutic effect. The results demonstrated the synergistic enhancement effect of TB@PMP compared to using PDT or chemotherapy only.
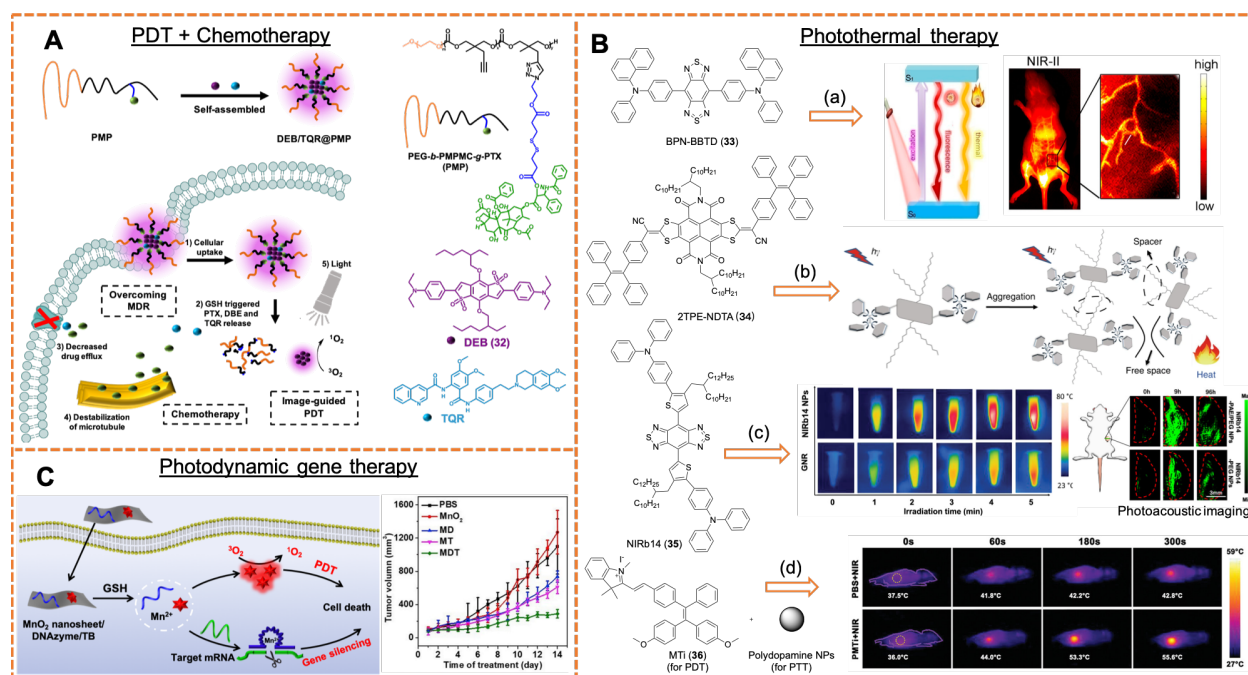
Figure 9. Combinational therapy based on AIE-PS. (A) Preparation process of DEB/TQR@PMP micelles and its internalization for PDT and chemotherapy for combating multi-drug resistant

(MDR) cancers. Reproduced from ref (60). Copyright 2019 Elsevier Ltd. (B) Structures of PTT active AIEgens. a) Illustration of single molecule NIR-II emitting BPN-BBTD NPs for fluorescence imaging and PTT. Deep tissue imaging was achieved on mice being injected with BPN-BBTD NPs under 785 nm irradiation. Reproduced from ref (62). Copyright 2018 American Chemical Society. b) Proposed working mechanism of 2TPE-NDTA for PTT: bulky sidechain allows active molecular motions in aggregate state to convert photo energy to heat. Reproduced from ref (63). Copyright 2019 Springer Nature. c) IR thermal images of NIRb14 NPs and GNRs under 808 nm laser irradiation for different durations. Photoacoustic imaging of mice being injected with NIRb14 NPs in different polymer matrix. Reproduced from ref (64). Copyright 2019 American Chemical Society. d) IR thermal images of tumor-bearing mice injected with either PBS as control or PMTi irradiated with 808 nm laser. Reproduced from ref (65). Copyright 2019 John Wiley & Sons, Inc. (C) Schematic illustration of MnO_2-DNAzyme-TB for gene silencing and PDT at the same time and their corresponding tumor volumes after different treatment by intratumoural injection. Reproduced from ref (68). Copyright 2019 Elsevier B.V.

A similar approach was adapted in a drug co-deliver system based on the reduction sensitive paclitaxel-releasing polymers (**Figure 9A**). NIR AIEgen (DEB, **32**)[60] with a quantum yield as high as 12.9% in the solid state was used as the PS together with a drug resistance inhibitor tariquidar (TQR) captured in the nanosystem. TQR is a P-glycoprotein inhibitor that blocks the efflux pump responsible for transporting anticancer drugs out of the target cells and which confers multidrug resistance during cancer therapy. The resulting DEB/TQR@PMP micelles exhibited a prominent synergistic lethal effect of PDT and chemotherapy. 12 h after injection to the mice, the micelles were effectively absorbed by tumor tissues without metabolism, as observed by DEB fluorescence signals. The micelles displayed enhanced inhibition of not only cancer cells but also

multi-drug resistant tumor growth. Both vascular and cellular effects contributed to PDT and chemotherapy efficacy can be affected by the drug-light interval. The results indicated the feasibility of combining PDT and chemotherapy can compensate for each other's weaknesses to enhance the treatment effect to a certain extent.

AIE-PS nanoparticles for photodynamic and photothermal therapy. Photothermal therapy (PTT) that transfers NIR light to thermal energy to produce hyperthermia that subsequently causes cell death has been used as another noninvasive modality for cancer treatment. The development of nanotechnology allows easy fabrication of a nanoplatform to combine PTT with PDT, which has been found to further enhance the therapeutic efficiency for malignant cancer treatment thanks to the synergistic effects. For example, Liu and coworkers reported a Cu(II)-aptamer complex[61] functionalized gold nanoparticles (GNP) for the combinational treatment for hepatocellular carcinoma. The aggregation of GNP in the tumor microenvironment enabled the photothermal ablation of cancer cells. The combination of Ce6, a classic PDT PS, with GNP demonstrated the advantage of such an approach for cancer therapy. However, most of the developed photoabsorbing agents for PTT are either inorganic materials that are hard to decompose and pose potential toxicity in a living system, or a large flat disc-like organic molecules that tend to aggregate with diminished therapeutic efficiency. New photoabsorbing agents that can overcome these problems and simultaneously produce multiple therapeutic modalities to generate a synergetic effect are in high demand.

AIE PSs with an emission wavelength located in the NIR-II region (1000-1700 nm) could fulfill this requirement and the non-radiative decay of the fluorogen could be harvested for PTT. Qian, Tang et al. reported a PTT system based on organic NPs with NIR-II-emitting BPN-BBTD (**33**)[62] as the PS encapsulated in the polymer Pluronic F-127 (**Figure 9B-a**). After excitation at 785

nm excitation, the emission of BPN-BBTD ranged from 800 to 1300 nm with an excellent fluorescence quantum yield of ~1.8% in the NIR-II window. Accompanying its light emission, the NPs exhibited high efficiency in photothermal conversion (39.8%) that allowed long-term whole-body tracing, deep tissue imaging and image-guided PTT of subcutaneous and orthotopic bladder tumor in mice.

The conversion of photon to thermal energy also makes photothermal materials promising for photoacoustic imaging, which detects the photothermally generated ultrasound signal for deep tissue imaging with high spatial resolution. Ding and Tang proposed a new molecular design strategy to generate effective excited-state intramolecular motion in the aggregate state within nanoparticles in order to promote non-radiative decay to increase photothermal conversion. 2TPE-NDTA (**34**)[63] consists of TPE units conjugated with a strong acceptor based on a naphthalene diimide to achieve a large π-conjugation, long wavelength absorption and high molar absorptivity. The long alkyl chains spatially isolated the fluorophores and provided a large space to enable free intramolecular motions such as rotation and vibration even in the aggregate and solid states (**Figure 9B-b**). Therefore, the resulting NPs with active intrinsic intramolecular motions showed almost no fluorescence but excellent photothermal conversion efficiency, indicating that the absorbed energy was efficiently harvested for heat generation. The NPs were applied for in vivo photoacoustic imaging that revealed tumor site in mice with high contrast 4 h post-injection. The results suggested the potential of harnessing molecular motion for cancer diagnosis.

Later on, Tang, Ding and coworkers made use of such molecular motions in aggregates for cancer theranostics. A series of molecular rotors with a planar donor-acceptor-donor alignment was decorated with alkyl chains of different length and geometry, and their effects on photothermal conversion were investigated. NIRb14 (**35**)[64] with the longest and branched alkyl chain displayed

the best photothermal conversion capacity and highest photothermal temperature elevation than the counterparts with short branched chains or linear chains as well as the widely used gold nanorods (GNR) (**Figure 9B-c**). NIRb14 was then encapsulated into mixed shell polymeric NPs that showed prolonged blood circulation, an enhanced EPR effect and improved tumor retention, that not only allowed the visualization of the tumor region through photoacoustic imaging but also enabled in vivo PTT with superb efficacy.

To combine PTT with PDT, Wang and Zhang developed a nanoplatform combining MTi (**36**)[65], an AIE PS for PDT, with polydopamine on the surface for PTT (**Figure 9B-d**). Polydopamine has strong absorbance in the NIR region and high photothermal energy conversion efficiency.[66] With the help of the positively charged indolium, MTi could target and image mitochondria. To improve the water solubility and retention in tumors, PEG was used together with polydopamine as a biocompatible matrix to stabilize AIEgens and keep their photosensitivity profile. The resulting nanoparticle, PMTi, was evaluated on cancer cells in vitro expressed a low IC_{50}, and in vivo where it suppressed the tumor growth rate and volume in mice, through the synergistic effect of PDT and PTT activated by white light and NIR laser source respectively.

AIE-PS nanoparticles for photodynamic gene therapy. RNA interference (RNAi) is a powerful gene-silencing methodology that holds great potential in the field of cancer therapy. The technology allows the rapid identification of key molecules and regulates the expression of key genes involved in many disease processes. The latter can be translated into therapeutic applications including for cancer treatment. Photodynamic gene therapy by combining both gene therapy and PDT therapy has emerged as an effective strategy to improve therapeutic effectiveness.

One of the challenges for PDT is the stress response of cancer cells, in which the level of vascular endothelial growth factor (VEGF) is upregulated to induce angiogenesis in order to suppress cellular senescence. This process significantly attenuates the PDT therapeutic effects. To suppress VEGF expression, a small interfering RNA (siRNA), siVEGF, can be used. However, the delivery of siRNA to the tumor cells is usually challenging because of its poor stability in the biological environment. To combat these challenges, Li et al. introduced a multifunctional theranostic NPs with AIE-active TTD (**25**)[67] embedded as the PS and surface modification by cRGD and siVEGF. The siVEGF was linked via a GSH cleavable disulfide bond. Upon recognizing integrin-overexpressing cancer cells, the NPs can be internalized and the siRNA on the surface would be cleaved in the reducing environment of the tumor cell as the result of elevated GSH level. Results showed that the expression level of both the VEGF protein and mRNA were downregulated when the cells were treated with the NPs. Cytotoxicity assays also revealed that the phototoxicity of the NPs towards the integrin overexpressing cell lines such as MDA-MB-231 were much higher than to those with low integrin expression levels (e.g. MCF-7, SK-BR-3).

Xia, Lou and coworkers developed a GSH responsive MnO_2 nanosheet to deliver the AIE-PS TB (**31**)[68] and a DNA enzyme (DNAzyme) for image-guided photodynamic gene therapy. In this approach, TB and DNAzyme were adsorbed onto MnO_2 nanosheets, which can be degraded when MnO_2 is reduced to Mn^{2+} in the presence of a high concentration of GSH (**Figure 9C**). Upon degradation, TB was released and aggregated in the hydrophilic intracellular milieu to produce intense red fluorescence and generate ROS. In the meantime, the released Mn^{2+} can serve as a cofactor for the DNAzyme and activate its catalytic activity to degrade the targeted mRNA to achieve gene knockdown. This approach was used to knockdown the early growth response-1 (EGR-1) gene to inhibit cell growth. The results shown that EGR-1 mRNA levels as well as protein

expression were effectively suppressed. This combination of therapeutic agents can thus improve the PDT therapeutic effect, especially in conditions associated with tumor hypoxia.

CONCLUSION AND PROSPECTS

As a noninvasive treatment, photodynamic therapy has been extensively studied for both cancer diagnosis and therapy. Notably, the therapeutic effect of PDT is directly influenced by the ROS generation ability of photosensitizers. The emerging aggregation-induced emission photosensitizers (AIE-PSs) and their application for image-guided therapy have attracted much attention. Both the fluorescence and $^1O_2$ generation ability of AIE-PSs are boosted upon aggregate formation. Through rational design, such processes can be activated under specific conditions that differentiate cancer cells from normal cells. In this perspective, we have summarized the approaches used to design effective AIE-PSs to achieve high phototoxicity to cancer cells and low toxicity to normal tissues in the dark. These approaches range from structural design of individual molecules to target specific organelles and generate ROS locally to manipulate pathways that lead to cell death, structural modification of AIE-PSs and fabrication of nanostructures with different groups such as peptide, drug, and polymers to improve their biostability, controllability and specificity. Lastly, we have exemplified the ensembles of multifunctional AIE-PSs to achieve combinational therapy, e.g. with chemo-, photothermal-, or gene therapy, to combat multidrug resistance and stress response of tumors from using single treatment modality. Even with the recent studies of AIE-PSs in cancer theranostics, there are still challenges and perhaps future opportunities to further advance AIE-PS for real-world applications. We summarize a few points as follows:

1. Because of insufficient luminous flux and peripheral normal tissue damage, the application of PDT is facing limitations especially in deep tumor therapy. This could possibly be overcome by precise molecular engineering to build molecules with different geometry to promote intersystem crossing for efficient ROS generation and to achieve ultrabright NIR emission[69] especially in the NIR-II window[70]. Rational structural design with the aid of theoretical study is highly desirable. Combination with multiphoton excitation or fluorescence microendoscopy with minimal invasion would be alternative approaches for AIE PSs to achieve deep tissue imaging and theranostics at cellular levels in vivo.

2. Integrating PDT with other treatment modalities offers high potential to enhance therapeutic effectiveness. For example, using PDT to assist tumor removal surgery could improve the accuracy of the surgery and lower the recurrence risk.[71] With novel functionalization at the molecular level and/or via nanoassembly being continually discovered, targeted cancer therapy by AIE-PSs can be further strengthened. Approaches such as linking AIE-PSs with tumor-associated biomarkers (peptide, antibody, oligonucleotide, small molecules, etc.)[72] can be employed to enhance the uptake and intracellular accumulation in tumors and cancer cells over normal healthy tissues.

3. Immune response during and after PDT with AIE-PS should be carefully studied. Immunogenic cell death caused by PDT can be harnessed to prime cancer immunotherapy to enhance the response rates.[73-75] In addition to apoptosis and necrosis, modulating other cell death and survival pathways such as autophagy, pyroptosis, the unfolded protein response, etc. might represent new opportunities to be explored to further improve the therapeutic effectiveness.

4. We also suggest practical improvement in the field of AIE-PS mediated PDT. In regard to different types of tumors at their different stages, such as primary cancers, metastatic cancers[76, 77],

of various organs and sites, we should design the corresponding AIE-PS and their nanocarrier to achieve better treatment results.[78] Changing some conditions during PDT treatment, such as optimizing the drug-light interval, should be also considered to improve the treatment efficiency.

In summary, we present the advantages, limitations and future directions for AIE-PSs, which are still at the infant stage for PDT of cancer. Although much effort and innovation are still needed on systematic investigation of the mechanisms and applications of PDT in cancer treatment[15,79–81], we believe that AIE-PSs could provide new opportunities to improve traditional PDT. We are hoping, through this perspective, to stimulate collaborative research interests from medicinal chemistry to develop new strategies to reinforce PDT in cancer therapy.

AUTHOR INFORMATION

Corresponding Author

*Email: Y.Hong@latrobe.edu.au (Y.H.) or louxiaoding@cug.edu.cn (X.L)

Author Contributions

[#]These authors contributed equally. The manuscript was written through contributions of all authors. All authors have given approval to the final version of the manuscript.

Biographies

Jun Dai completed his PhD in 2016 at Huazhong University of Science and Technology (HUST) under the supervision of Prof Qiurong Ruan. In 2016, he joined the Department of Obstetrics and Gynecology, Tongji Hospital, Tongji Medical College, HUST, and served as an attending physician. His scientific interest is focused on biomedical engineering.

Xia Wu obtained her BSc in 2015 from China Pharmaceutical University and MSc in 2018 from Chongqing University. Currently she is a PhD student in the group of Prof Xiaoding Lou at China University of Geosciences, Wuhan, China.

Siyang Ding is a PhD student in Dr Yuning Hong's group at La Trobe University. She obtained her BEng in Materials Science and Engineering in 2017 from South China University of Technology (SCUT), Guangzhou, China. Proceeding from the background of organic functional materials under the supervision of Prof Zujin Zhao in SCUT, her current project in Dr Hong's group is focused on constructing novel synthetic biosensors and methodologies for neurodegenerative disease-related applications.

Xiaoding Lou received her Ph.D. in organic chemistry from Wuhan University in 2012 under the supervision of Prof Zhen Li. She then worked as a Research Associate in Prof Ben Zhong Tang's group at the Hong Kong University of Science and Technology. In 2013 she joined HUST as Assistant Professor. In 2016 she worked in the group of Prof Alan J. Heeger at University of California, Santa Barbara, CA. Since 2017, she is appointed as a Professor of Analytical Chemistry at China University of Geosciences. Her scientific interest is focused on the chemical and biological sensor field.

Fan Xia studied Physical Chemistry at the Institute of Chemistry, Chinese Academy of Sciences and received his PhD in 2008 under the supervision of Prof Lei Jiang. He then worked as a postdoctoral scholar with Profs Alan J. Heeger, Kevin Plaxco, and Herb Waite at the University of California, Santa Barbara, CA. He joined HUST as a Professor in 2012. Currently he is a Professor and Dean of Faculty of Materials Science and Chemistry, China University of Geosciences, Wuhan. His scientific interest is focused on bioanalytical chemistry.

Shixuan Wang was graduated as a medical doctor from Sun Yet-san University of Medical Science in 1988. Then he was allocated to work in Tongji Hospital and awarded his PhD degree in 1996. In 2002, Dr Wang went to Southwestern Medical Center of Texas University at Dallas for his postdoctoral training. After two years' training, he returned to China and joined the team of Prof Ding Ma and was appointed as a Professor, Vice Chairman of Department of Obstetrics and Gynecology and Chief in Department of Gynecology at Tongji Hospital since 2005. In addition to his profound attainments in cancer research, Prof Wang and his team are also interested in ovarian aging.

Yuning Hong received her BSc in Applied Chemistry (2006) from Sun Yat-sen University, China and PhD in Nano Science and Technology (2011) from Hong Kong University of Science and Technology (HKUST) under the supervisor of Prof Ben Zhong Tang. She held postdoctoral positions in Prof Ekaterina V. Pletneva's group at Dartmouth College, NH, as Research Assistant Professor in HKUST, and as McKenzie Fellow in University of Melbourne. She joined La Trobe University in 2016 and is currently a Senior Lecturer in the Department of Chemistry and Physics, La Trobe University, Australia. Her research interests focus on chemical biology of proteostasis for disease diagnosis and treatment.

ACKNOWLEDGMENT

ABBREVIATIONS

$^1O_2$, singlet oxygen; 2PA, two-photon absorption; $^3O_2$, triplet oxygen; ABDA, 9,10-anthracenediyl-bis(methylene)dimalonic acid; ACQ, aggregation-caused quenching; AIE, aggregation-induced emission; AIEgens, AIE fluorogens; AIE-PSs, aggregation-induced emission photosensitizers; ART, Artmisinin; CD13, aminopeptidase N; CPP, cell-penetrating peptide; Cor-PEG, corannulene-decorated PEG; cRGD tag, the cyclic RGD peptide; DEVD peptide, -Asp-Glu-Val-Asp-; DNAzyme, DNA enzyme; DNBS, 2,4-dinitrobenzenesulfonyl; DOX, doxorubicin; DSPE-PEG, 1,2-Distearoyl-*sn*-glycero-3-phosphoethanolamine-*N*-[methoxy(polyethylene glycol)-2000]; DSPE-PEG-Mal, 1,2-distearoyl-*sn*-glycerol-3-phosphoethanolamine-*N*-[maleimide(polyethylene glycol)]; EGR-1, early growth response-1; EPR, enhanced permeability and retention effect; ER, endoplasmic reticulum; FDA, fluorescein diacetates; FR, folate receptors; GFLG, -Gly-Phe-Leu-Gly-; GNP, gold nanoparticles; GSH, glutathione; LAPTM4B, lysosomal protein transmembrane 4 beta; LDs, lipid droplets; LGLAG, MMP-2 responsive peptide; MMC, Mitomycin C; Cbl, Chlorambucil; MMP-2, Matrix metalloproteinase-2; NGR, Asn-Gly-Arg; NIR, near infra-red; NLS peptide, nuclear localization signal; PCNA, proliferating cell nuclear antigen; PDT, photodynamic therapy; PEG, polyethylene glycol; PI, propidium iodine; PS, photosensitizer; PSs, photosensitizers; RGD, Arg-Gly-Asp; RIM/RIR, intramolecular motions/rotations; RNAi, RNA interference; ROS, reactive oxygen species; S_0, the ground state; S_1, the lowest excited singlet state; T_1, the excited triplet state; TPE, tetraphenylethene; TPP, triphenylpholinium; TQR, tariquidar; VEGF, vascular endothelial growth factor

REFERENCES

(1)   Gotwals, P.; Cameron, S.; Cipolletta, D.; Cremasco, V.; Crystal, A.; Hewes, B.; Mueller, B.; Quaratino, S.; Sabatos-Peyton, C.; Petruzzelli, L. Prospects for Combining Targeted and Conventional Cancer Therapy with Immunotherapy. *Nat. Rev. Cancer* **2017**, *17*, 286-301.

(2)   Dougherty, T. J.; Gomer, C. J.; Henderson, B. W.; Jori, G.; Kessel, D.; Korbelik, M.; Moan, J.; Peng, Q. Photodynamic Therapy. *J. Natl. Cancer Inst.* **1998**, *90*, 889-905.

(3)   Zhou, Z.; Song, J.; Nie, L.; Chen, X. Reactive Oxygen Species Generating Systems Meeting Challenges of Photodynamic Cancer Therapy. *Chem. Soc. Rev.* **2016**, *45*, 6597-6626.

(4)   Celli, J. P.; Spring, B. Q.; Rizvi, I.; Evans, C. L.; Samkoe, K. S.; Verma, S.; Pogue, B. W.; Hasan, T. Imaging and Photodynamic Therapy: Mechanisms, Monitoring, and Optimization. *Chem. Rev.* **2010**, *110*, 2795-2838.

(5)   Kataoka, H.; Nishie, H.; Hayashi, N.; Tanaka, M.; Nomoto, A.; Yano, S.; Joh, T. New Photodynamic Therapy with Next-Generation Photosensitizers. *Ann. Transl. Med.* **2017**, *5*, 183.

(6)   Kriegmair, M.; Baumgartner, R.; Knuchel, R.; Stepp, H.; Hofstadter, F.; Hofstetter, A. Detection of Early Bladder Cancer by 5-Aminolevulinic Acid Induced Porphyrin Fluorescence. *J. Urol.* **1996**, *155*, 105-110.

(7)   Nseyo, U. O.; Shumaker, B.; Klein, E. A.; Sutherland, K. Photodynamic Therapy Using Porfimer Sodium as an Alternative to Cystectomy in Patients with Refractory Transitional Cell Carcinoma in Situ of the Bladder. Bladder Photofrin Study Group. *J. Urol.* **1998**, *160*, 39-44.

(8)   Bonnett, R. Photosensitizers of the Porphyrin and Phthalocyanine Series for Photodynamic Therapy. *Chem. Soc. Rev.* **1995**, *24*, 19-33.

(9)   Wang, H.-Y.; Blaszczyk S. A.; Xiao, G.; Tang, W. Chiral Reagents in Glycosylation and Modification of Carbohydrates. *Chem. Soc. Rev.* **2018**, *47*, 681-701.

(10)   Lin F.-J.; Chen H.-H.; Tao Y.-T. Molecularly Aligned Hexa-peri-hexabenzocoronene Films by Brush-Coating and Their Application in Thin-Film Transistors. *ACS Appl. Mater. Interfaces* **2019**, *11*, 10801-10809.

(11)   Hong, Y.; Lam, J. W. Y.; Tang, B. Z. Aggregation-Induced Emission: Phenomenon, Mechanism and Applications. *Chem. Commun.* **2009**, *29*, 4332-4353.

(12)   Luo, J.; Xie, Z.; Lam, J. W.; Cheng, L.; Chen, H.; Qiu, C.; Kwok, H. S.; Zhan, X.; Liu, Y.; Zhu, D.; Tang, B. Z. Aggregation-Induced Emission of 1-Methyl-1,2,3,4,5-Pentaphenylsilole. *Chem. Commun.* **2001**, *18*, 1740-1741.

(13)   Qian, J.; Tang, B. Z. AIE Luminogens for Bioimaging and Theranostics: From Organelles to Animals. *Chem* **2017**, *3*, 56-91.

(14)   Hogue, C. W.; MacManus, J. P.; Banville, D.; Szabo, A. G. Comparison of Terbium (III) Luminescence Enhancement in Mutants of EF Hand Calcium Binding Proteins. *J. Biol. Chem.* **1992**, *267*, 13340-13347.

(15)   Hu, F.; Xu, S.; Liu, B. Photosensitizers with Aggregation-Induced Emission: Materials and Biomedical Applications. *Adv. Mater.* **2018**, *30*, 1801350.

(16)   Zhao, J.; Wu, W.; Sun, J.; Guo, S. Triplet Photosensitizers: From Molecular Design to Applications. *Chem. Soc. Rev.* **2013**, *42*, 5323-5351.

(17)   Kang, M.; Zhou, C.; Wu, S.; Yu, B.; Zhang, Z.; Song, N.; Lee, M. M. S.; Xu, W.; Xu, F. J.; Wang, D.; Wang, L.; Tang, B. Z. Evaluation of Structure-Function Relationships of

Aggregation-Induced Emission Luminogens for Simulataneous Dual Application of Specific Discrimination and Efficient Photodynamic Killing of Gram-Positive Bacteria. *J. Am. Chem. Soc.* **2019**, *141*, 16781-16789.

(18)   Mroz, P.; Yaroslavsky, A.; Kharkwal, G. B.; Hamblin, M. R. Cell Death Pathways in Photodynamic Therapy of Cancer. *Cancers*, **2011**, *3*, 2516-2539.

(19)   Marchi, S.; Giorgi, C.; Suski, J. M.; Agnoletto, C.; Bononi, A.; Bonora, M.; De Marchi, E.; Missiroli, S.; Patergnani, S.; Poletti, F.; Rimessi, A.; Duszynski, J.; Wieckowski, M. R.; Pinton, P. Mitochondria-Ros Crosstalk in the Control of Cell Death and Aging. *J. Signal Transduct.* **2012**, *2012*, 329635.

(20)   Nishikawa, T.; Araki, E. Impact of Mitochondrial ROS Production in the Pathogenesis of Diabetes Mellitus and Its Complications. *Antioxid. Redox Signal.* **2007**, *9*, 343-353.

(21)   Wang, D.; Lee, M. M. S.; Shan, G.; Kwok, R. T. K.; Lam, J. W. Y.; Su, H.; Cai, Y.; Tang, B. Z. Highly Efficient Photosensitizers with Far-Red/Near-Infrared Aggregation-Induced Emission for In Vitro and In Vivo Cancer Theranostics. *Adv. Mater.* **2018**, *30*, 1802105.

(22)   Zhang, T.; Li, Y.; Zheng, Z.; Ye, R.; Zhang, Y.; Kwok, R. T. K.; Lam, J. W. Y.; Tang, B. Z. In Situ Monitoring Apoptosis Process by a Self-Reporting Photosensitizer. *J. Am. Chem. Soc.* **2019**, *141*, 5612-5616.

(23)   You, X.; Ma, H.; Wang, Y.; Zhang, G.; Peng, Q.; Liu, L.; Wang, S.; Zhang, D. Pyridinium-Substituted TetraphenylethyleneEntailing Alkyne Moiety: Enhancement of Photosensitizing Efficiency and Antimicrobial Activity. *Chem. Asian J.* **2017**, *12*, 1013-1019.

(24)   Yang, C.; Hu, R.; Lu, F.; Guo, X.; Wang, S.; Zeng, Y.; Li, Y.; Yang, G. Traceable Cancer Cell Photoablation with a New Mitochondria-Responsive and -Activatable Red-Emissive Photosensitizer. *Chem. Commun.* **2019**, *55*, 3801-3804.

(25)   Zou, J.; Lu, H.; Zhao, X.; Li, W.; Guan, Y.; Zheng, Y.; Zhang, L. Dyes and Pigments A Multi-Functional Fluorescent Probe with Aggregation-Induced Emission Characteristics : Mitochondrial Imaging , Photodynamic Therapy and Visualizing Therapeutic Process in Zebra Fi Sh Model. *Dye. Pigment.* **2018**, *151*, 45-53.

(26)   Zhang, W.; Huang, Y.; Chen, Y.; Zhao, E.; Hong, Y.; Chen, S.; Lam, J. W. Y.; Chen, Y.; Hou, J.; Tang, B. Z. Amphiphilic Tetraphenylethene-Based Pyridinium Salt for Selective Cell-Membrane Imaging and Room-Light-Induced Special Reactive Oxygen Species Generation. *ACS Appl. Mater. Interfaces* **2019**, *11*, 10567-10577.

(27)   Petan, T.; Jarc, E.; Jusovic, M. Lipid Droplets in Cancer: Guardians of Fat in a Stressful World. *Molecules* **2018**, *23*, 1900-1941.

(28)   Shyu, P. J.; Wong, X. F. A.; Crasta, K.; Thibault, G. Dropping in on Lipid Droplets: Insights into Cellular Stress and Cancer. *Biosci. Rep.* **2018**, *38*, BSR20180764.

(29)   Xu, W.; Lee, M. M. S.; Lee, M. M. S.; Zhang, Z.; Sung, H. H. Y.; Williams, I. D.; Kwok, R. T. K.; Tang, B. Z. Chemical Science Facile Synthesis of AIEgens with Wide Color Tunability for Cellular Imaging and Therapy. *Chem. Sci.* **2019**, *10*, 3494-3501.

(30)   Zhou, Y.; Cheung, Y.-K.; Ma, C.; Zhao, S.; Gao, D.; Lo, P.-C.; Fong, W.-P.; Wong, K. S.; Ng, D. K. P. Endoplasmic Reticulum-Localized Two-Photon-Absorbing Boron Dipyrromethenes as Advanced Photosensitizers for Photodynamic Therapy. *J. Med. Chem.* **2018**, *61*, 3952-3961.

(31) Albota, M.; Beljonne, D.; Bredas, J. L.; Ehrlich, J. E.; Fu, J. Y.; Heikal, A. A.; Hess, S. E.; Kogej, T.; Levin, M. D.; Marder, S. R.; Maughin, D. M.; Pery, J.M.; Rockel, H.; Rumi, M.; Subramaniam, G.; Webb, W. W.; Wu, X. L.; Xu, C. Design of Organic Molecules with Large Two-Photon Absorption Cross Sections. *Science* **1998**, *281*, 1653-1656.

(32) Jiang, M.; Kwok, R. T. K.; Li, X.; Gui, C.; Lam, J. W. Y.; Qu, J.; Tang, B. Z. A Simple Mitochondrial Targeting AIEgen for Image-Guided Two-Photon Excited Photodynamic Therapy. *J. Mater. Chem. B* **2018**, *6*, 2557-2565.

(33) Liu, J.; Jin, C.; Yuan, B.; Liu, X.; Chen, Y.; Ji, L.; Chao, H. Selectively Lighting up Two-Photon Photodynamic Activity in Mitochondria with AIE-Active Iridium(Iii) Complexes. *Chem. Commun.* **2017**, *53*, 2052-2055.

(34) Cheng, Y.; Sun, C.; Ou, X.; Liu, B.; Lou, X.; Xia, F. Dual-Targeted Peptide-Conjugated Multifunctional Fluorescent Probe with AIEgen for Efficient Nucleus-Specific Imaging and Long-Term Tracing of Cancer Cells. *Chem. Sci.* **2017**, *8*, 4571-4578.

(35) Yuan, Y.; Xu, S.; Zhang, C.-J.; Zhang, R.; Liu, B. Dual-Targeted Activatable Photosensitizers with Aggregation-Induced Emission (AIE) Characteristics for Image-Guided Photodynamic Cancer Cell Ablation. *J. Mater. Che*m. *B* **2016**, *4*, 169-176.

(36) Yuan, Y.; Zhang, C. J.; Kwok, R. T. K.; Xu, S.; Zhang, R.; Wu, J.; Tang, B. Z.; Liu, B. Light-Up Probe for Targeted and Activatable Photodynamic Therapy with Real-Time in Situ Reporting of Sensitizer Activation and Therapeutic Responses. *Adv. Funct. Mater.* **2015**, *25*, 6586-6595.

(37) Choi, K. Y.; Swierczewska, M.; Lee, S.; Chen, X. Protease-Activated Drug Development. *Theranostics* **2012**, *2*, 156-178.

(38)   Yuan, Y.; Zhang, C.; Gao, M.; Zhang, R.; Tang, B. Z.; Liu, B. Specific Light-Up Bioprobe with Aggregation-Induced Emission and Activatable Photoactivity for the Targeted and Image-Guided Photodynamic Ablation of Cancer Cells. *Angew. Chem., Int. Ed.* **2015**, *54*, 1780-1786.

(39)   Cheng, Y.; Huang, F.; Min, X.; Gao, P.; Zhang, T.; Li, X.; Liu, B.; Hong, Y.; Lou, X.; Xia, F. Protease-Responsive Prodrug with Aggregation-Induced Emission Probe for Controlled Drug Delivery and Drug Release Tracking in Living Cells. *Anal Chem.* **2016**, *88*, 8913-8919

(40)   Liu, X.; Liang, G. Dual Aggregation-Induced Emission for Enhanced Fluorescence Sensing of Furin Activity in Vitro and in Living Cells. *Chem. Commun.* **2017**, *53*, 1037-1040.

(41)   Hu, F.; Huang, Y.; Zhang, G.; Zhao, R.; Yang, H.; Zhang, D. Targeted Bioimaging and Photodynamic Therapy of Cancer Cells with an Activatable Red Fluorescent Bioprobe. *Anal Chem.* **2014**, *86*, 7989-7995.

(42)   Hu, F.; Yuan, Y.; Mao, D.; Wu, W.; Liu, B. Biomaterials Smart Activatable and Traceable Dual-Prodrug for Image-Guided Combination Photodynamic and Chemo-Therapy. *Biomaterials* **2017**, *144*, 53-59.

(43)   Parthiban, C.; Pavithra, M.; Reddy, L. V. K.; Sen, D.; Singh, N. D. P. Single-Component Fluorescent Organic Nanoparticles with Four-Armed Phototriggers for Chemo-Photodynamic Therapy and Cellular Imaging. *ACS Appl. Nano Mater.* **2019**, *2*, 3728-3734.

(44)   Feng, G.; Liu, J.; Zhang, C.; Liu, B. Artemisinin and AIEgen Conjugate for Mitochondria-Targeted and Image-Guided Chemo- and Photodynamic Cancer Cell Ablation. *ACS Appl Mater Interfaces.* **2018**, *10*, 11546-11553.

(45)   Chen, X.; Li, Y.; Li, S.; Gao, M.; Ren, L.; Tang, B. Z. Mitochondria-and Lysosomes-Targeted Synergistic Chemo-Photodynamic Therapy Associated with Self-Monitoring by Dual Light-Up Fluorescence. *Adv. Funct. Mater.* **2018**, *28*, 1804362.

(46)   Guan, Y.; Lu, H.; Li, W.; Zheng, Y.; Jiang, Z.; Zou, J.; Gao, H. Near-Infrared Triggered Upconversion Polymeric Nanoparticles Based on Aggregation-Induced Emission and Mitochondria Targeting for Photodynamic Cancer Therapy. *ACS Appl Mater Interfaces.* **2017**, *9*, 26731-26739.

(47)   Wang, S.; Wu, W.; Manghnani, P.; Xu, S.; Wang, Y.; Goh, C. C.; Ng, L. G.; Liu, B. Polymerization-Enhanced Two-Photon Photosensitization for Precise Photodynamic Therapy. *ACS Nano* **2019**, *13*, 3095-3105.

(48)   Rizzuti, M.; Nizzardo, M.; Zanetta, C.; Ramirez, A.; Corti, S. Therapeutic Applications of the Cell-Penetrating HIV-1 Tat Peptide. *Drug Discov. Today* **2015**, *20*, 76-85.

(49)   Wu, W.; Mao, D.; Hu, F.; Xu, S.; Chen, C.; Zhang, C.; Cheng, X.; Yuan, Y.; Ding, D.; Kong, D. Liu, B. A Highly Efficient and Photostable Photosensitizer with Near-Infrared Aggregation-Induced Emission for Image-Guided Photodynamic Anticancer Therapy. *Adv. Mater.* **2017**, *29*, 1700548.

(50)   Gu, B.; Wu, W.; Xu, G.; Feng, G.; Yin, F.; Han, P.; Chong, J.; Qu, J.; Yong, K.; Liu, B. Precise Two-Photon Photodynamic Therapy Using an Efficient Photosensitizer with Aggregation-Induced Emission Characteristics. *Adv. Mater.* **2017**, *29*, 1701076.

(51)   Zhang, L.; Li, Y.; Che, W.; Zhu, D.; Li, G.; Xie, Z.; Song, N.; Liu, S.; Tang, B. Z.; Liu, X.; Su, Z.; Bryce, M. R. AIE Multinuclear Ir(III) Complexes for Biocompatible Organic Nanoparticles with Highly Enhanced Photodynamic Performance. *Adv. Sci.* **2019**, *6*, 1802050.

(52)   Yuan, Y.; Feng, G.; Qin, W.; Tang, B. Z.; Liu, B. Targeted and Image-guided Photodynamic Cancer Therapy based on Organic Nanoparticles with Aggregation-Induced Emission Charateristics. *Chem. Commun.* **2014**, *50*, 8757.

(53)   Li, M.; Gao, Y.; Yuan, Y.; Wu, Y.; Song, Z.; Tang, B. Z.; Liu, B.; Zheng, Q. C. One-Step Formulation of Targeted Aggregation-Induced Emission Dots for Image-Guided Photodynamic Therapy of Cholangiocarcinoma. *ACS Nano.* **2017**, *11*, 3922-3932.

(54)   Gao, Y.; Zheng, Q. C.; Xu, S.; Yuan, Y.; Cheng, X.; Jiang, S.; Kenry; Yu, Q.; Song, Z.; Liu, B.; Li. M. Theranostic Nanodots with Aggregation-Induced Emission Characteristic for Targeted and Image-Guided Photodynamic Therapy of Hepatocellular Carcinoma. *Theranostics* **2019**, *9*, 1264-1279.

(55)   Feng, G.; Qin, W.; Hu, Q.; Tang, B. Z.; Liu, B. Cellular and Mitochondrial Dual-Targeted Organic Dots with Aggregation-Induced Emission Characteristics for Image-Guided Photodynamic Therapy. *Adv Healthc Mater* **2015**, *4*, 2667-2676.

(56)   Yang, Y.; Wang, L.; Cao, H.; Li, Q.; Li, Y.; Han, M.; Wang, H.; Li, J. Photodynamic Therapy with Liposomes Encapsulating Photosensitizers with Aggregation-Induced Emission. *Nano Lett.* **2019**, *19*, 1821-1826.

(57)   Gu, X.; Zhang, X.; Ma, H.; Jia, S.; Zhang, P.; Zhao, Y.; Liu, Q.; Wang, J.; Zheng, X.; Lam, J. W. Y. Ding, D; Tang, B. Z. Corannulene-Incorporated AIE Nanodots with Highly Suppressed Nonradiative Decay for Boosted Cancer Phototheranostics In Vivo. *Adv. Mater.* **2018**, *30*, 1801065.

(58)   Mao, D.; Wu, W.; Ji. S.; Chen, C.; Hu, F.; Kong, D.; Ding, D.; Liu, B. Chemiluminescence-Guided Cancer Therapy Using a Chemiexcited Photosensitizer Chemiluminescence-Guided Cancer Therapy Using a Chemiexcited Photosensitizer. *Chem* **2017**, *3*, 991-1007.

(59)   Yi, X.; Dai, J.; Han, Y.; Xu, M.; Zhang, X.; Zhen, S.; Zhao, Z.; Lou, X.; Xia, F. A High Therapeutic Efficacy of Polymeric Prodrug Nano-Assembly for a Combination of Photodynamic Therapy and Chemotherapy. *Commun Biol.* **2018**, *1*, 202.

(60)   Zhen, S.; Yi, X.; Zhao, Z.; Lou, X.; Xia, F.; Tang, B. Z. Biomaterials Drug Delivery Micelles with Efficient Near-Infrared Photosensitizer for Combined Image-Guided Photodynamic Therapy and Chemotherapy of Drug-Resistant Cancer. *Biomaterials* **2019**, *218*, 119330.

(61)   Zhang, D.; Zheng, A.; Li, J.; Wu, M.; Wu, L.; Wei, Z.; Liao, N.; Zhang, X.; Cai, Z.; Yang, H. Liu, G.; Liu, X.; Liu, J. Smart Cu(II)-Aptamer Complexes Based Gold Nanoplatform for Tumor Micro-Environment Triggered Programmable Intracellular Prodrug Release, Photodynamic Treatment and Aggregation Induced Photothermal Therapy of Hepatocellular Carcinoma. *Theranostics* **2017**, *7*, 164-179.

(62)   Alifu, N.; Zebibula, A.; Qi, J.; Zhang, H.; Sun, C.; Yu, X.; Xue, D.; Lam, J. W. Y.; Li, G.; Qian, J. Single-Molecular Near-Infrared-II Theranostic Systems: Ultrastable Aggregation-Induced Emission Nanoparticles for Long-Term Tracing and Efficient Photothermal Therapy. *ACS Nano* **2018**, *12*, 11282-11293.

(63)   Zhao, Z.; Chen, C.; Wu, W.; Wang, F.; Du, L.; Zhang, X.; Xiong, Y.; He, X.; Cai, Y.; Kwok, R. T. Gao, X.; Sun, P.; Phillips, D.; Ding, D.; Tang, B. Z. Highly Efficient Photothermal Nanoagent Achieved by Harvesting Energy via Excited-State Intramolecular Motion within Nanoparticles. *Nat. Commun.* **2019**, *10*, 768.

(64)   Liu, S.; Zhou, X.; Zhang, H.; Ou, H.; Lam, J. W. Y.; Liu, Y.; Shi, L.; Ding, D.; Tang, B. Z. Molecular Motion in Aggregates: Manipulating TICT for Boosting Photothermal Theranostics. *J. Am. Chem. Soc.* **2019**, *141*, 5359-5368.

(65)   Chen, Y.; Ai, W.; Guo, X.; Li, Y.; Ma, Y.; Chen, L.; Zhang, H.; Wang, T.; Zhang, X.; Wang, Z. Mitochondria-Targeted Polydopamine Nanocomposite with AIE Photosensitizer for Image-Guided Photodynamic and Photothermal Tumor Ablation. *Small* **2019**, *15*, 1902352.

(66)   Zhu, Z.; Su, M. Polydopamine Nanoparticles for Combined Chemo- and Photothermal Cancer Therapy. *Nanomater.* **2017**, *7*, 160.

(67)   Jin, G.; Feng, G.; Qin, W.; Tang, B. Z.; Liu, B.; Li, K. Multifunctional Organic Nanoparticles with Aggregation-Induced Emission (AIE) Characteristics for Targeted Photodynamic Therapy and RNA Interference Therapy. *Chem. Commun.* **2016**, *52*, 2752-2755.

(68)   Wang, X.; Dai, J.; Wang, X.; Hu, Q.; Huang, K.; Zhao, Z.; Lou, X.; Xia, F. MnO_2-DNAzyme-Photosensitizer Nanocomposite with AIE Characteristic for Cell Imaging and Photodynamic-Gene Therapy. *Talanta* **2019**, *202*, 591-599.

(69)   Zhang, R.; Duan, Y.; Liu, B. Recent Advances of AIE Dots in NIR Imaging and Phototherapy. *Nanoscale* **2019**, *11*, 19241-19250.

(70)   Li, C.; Wang, Q. Advanced NIR-II Fluorescence Imaging Technology for In Vivo Precision Tumor Theranostics. *Adv. Ther.* **2019**, *2*, 1900053.

(71)   O'Gorman, S. M.; Clowry, J.; Manley, M.; McCavana, J.; Gray, L.; Kavanagh, A.; Lally, A.; Collins, P. Artificial White Light vs Daylight Photodynamic Therapy for Actinic Keratoses: A Randomized Clinical Trial. *JAMA dermatol.* **2016**, *152*, 638-644.

(72)   Wu, F.; Wu, X.; Duan, Z.; Huang, Y.; Lou, X.; Xia, F. Biomacromolecule-Functionalized AIEgens for Advanced Biomedical Studies. *Small* **2019**, *15*, 1804839.

(73)   Liu, W.; Zou, M.; Liu, T.; Zeng, J.; Li, X.; Yu, W.; Li, C.; Ye, J.; Song, W.; Feng, J. Zhang, X. Expandable Immunotherapeutic Nanoplatforms Engineered from Cytomembranes of Hybrid Cells Derived from Cancer and Dendritic Cells. *Adv. Mater.* **2019**, *31*, 1900499.

(74)   Meng, Z.; Zhou, X.; Xu, J.; Han, X.; Dong, Z.; Wang, H.; Zhang, Y.; She, J.; Xu, L.; Wang, C. Liu, Z. Light-Triggered In Situ Gelation to Enable Robust Photodynamic-Immunotherapy by Repeated Stimulations. *Adv. Mater.* **2019**, *31*, 1900927.

(75)   Lan, G.; Ni, K.; Xu, Z.; Veroneau, S. S.; Song, Y.; Lin, W. Nanoscale Metal-organic Framework Overcomes Hypoxia for Photodynamic Therapy Primed Cancer Immunotherapy. *J. Am. Chem. Soc.* **2018**, *140*, 5670-5673.

(76)   Hajdu, S. I.; Urban, J. A. Cancers Metastatic to the Breast. *Cancer* **1972**, *29*, 1691-1696.

(77)   Penn, I. Hepatic Transplantation for Primary and Metastatic Cancers of the Liver. *Surgery* **1991**, *110*, 726-734.

(78)   Chen, Y.; Su, Y.; Hu, S.; Chen, S. Functionalized Graphene Nanocomposites for Enhancing Photothermal Therapy in Tumor Treatment . *Adv. Drug Deliv. Rev.* **2016**, *105*, 190-204.

(79)   Feng, G.; Liu, B. Aggregation-Induced Emission (AIE) Dots: Emerging Theranostic Nanolights. *Acc. Chem. Res.* **2018**, *51*, 1404-1414.

(80)   Gao, M.; Tang, B. Z. AIE-Based Cancer Theranostics. *Coord. Chem. Rev.* **2020**, *402*, 213076.

(81)   He, X.; Xiong, L.-H.; Zhao, Z.; Wang, Z.; Luo, L.; Lam, J. W. Y.; Kwok, R. T. K.; Tang, B. Z. AIE-Based Theranostic Systems for Detection and Killing of Pathogens. *Theranostics* **2019**, *9*, 3223.

Table of Contents graphic